



IMAGE ENHANCEMENT FOR UNDERWATER MINING APPLICATIONS

SHRAVAN DEV RAJESH

novembro de 2019

INSTITUTO SUPERIOR DE ENGENHARIA DO PORTO

Image Enhancement For Underwater Mining Applications

Shravan Dev Rajesh



Instituto Superior de
Engenharia do Porto

Masters In Electrical and Computer Engineering

Orientador: Alfredo Manuel Oliveira Martins

November 19, 2019

*“Went face to face with all our fears, Learned our lessons through the tears, Made
memories we knew would never fade”*

Tim Bergling: The Nights

**THIS PAGE
INTENTIONALLY
LEFT BLANK**

Abstract

The exploration of water bodies from the sea to land filled water spaces has seen a continuous increase with new technologies such as robotics. Underwater images is one of the main sensor resources used but suffer from added problems due to the environment. Multiple methods and techniques have provided a way to correct the color, clear the poor quality and enhance the features. In this thesis work, we present the work of an Image Cleaning and Enhancement Technique which is based on performing color correction on images incorporated with Dark Channel Prior (DCP) and then taking the converted images and modifying them into the Long, Medium and Short (LMS) color space, as this space is the region in which the human eye perceives colour. This work is being developed at LSA (Laboratorio de Sistema Autonomos) robotics and autonomous systems laboratory. Our objective is to improve the quality of images for and taken by robots with the particular emphasis on underwater flooded mines. This thesis work describes the architecture and the developed solution. A comparative analysis with state of the art methods and of our proposed solution is presented. Results from missions taken by the robot in operational mine scenarios are presented and discussed and allowing for the solution characterization and validation.

Keywords: Underwater Images, Image processing, Image enhancement, Color correction, Computer vision, Underwater robots, Underwater mining

**THIS PAGE
INTENTIONALLY
LEFT BLANK**

Acknowledgements

This dissertation would not have been possible if it was not for my mentor and guide Professor Alfredo Manuel Oliveira Martins who has guided me personally and professionally along the entire process to work harder and push further.

I would like to thank my Professor Luis Lima for always being open to listening to my troubles and be comforting with positive words and reassurance during times of stress and anxiety.

I would like to thank the entire department of Electrical and Computer Engineering: Autonomous Systems for passing on their knowledge and inspiring me to always strive for better even in the smallest things in life.

I would like to thank all my friends who I am grateful to have met, bonded and gotten to know, for not only helping me in academics and making this a journey to be kept close to my heart.

I would like to thank the people who have always believed in me, have had nothing but the best intentions for my life and I feel blessed that those people are part of my life.

Nobody has been more important to me in the pursuit of seeing me finish this course than the members of my family. I express my utmost gratitude to my parents, especially my mother, and to my grandmother for providing me with unfailing support, continuous inspiration and encouragement throughout my years of study and through the process of researching and writing this thesis.

This accomplishment would not have been possible without them. Thank you.

Shravan Dev Rajesh

**THIS PAGE
INTENTIONALLY
LEFT BLANK**

Contents

1	Introduction	13
1.1	Objectives	15
1.2	Thesis Structure	16
2	Problem Formulation	17
3	Related Work	23
4	Theoretical Background	27
4.1	Light Properties	27
4.2	Color Spaces	28
4.3	Formation of Images	34
4.4	Normalization	35
4.5	Dark Channel Prior	35
4.6	Robot Operating System	36
5	Design Solution	39
5.1	Color Correction	39
5.2	XYZ to LMS Conversion	40
5.3	Underwater Image Quality Measurement	41
6	Implementation	43
6.1	Color Correction	43
6.2	Dark Channel Prior	47
6.3	XYZ to LMS conversion	49
6.4	Integration in Robot Operating System-ROS	50
7	Results	51
8	Conclusion and Future Work	63
8.1	Conclusion	63
8.2	Future Work	63

**THIS PAGE
INTENTIONALLY
LEFT BLANK**

List of Figures

2.1	Mining Machine	18
2.2	Model of EVA [7]	19
2.3	Deployment of EVA at Lee Moor Mine, UK	19
2.4	Model of UX-1 [11]	21
2.5	UX-1 entering the Ecton mine, UK	21
2.6	UX-1 exploring Ecton mine	21
2.7	Mineral sample board placed in Idrija Mine	22
4.1	Dispersion of light underwater	27
4.2	Histogram Graph of the RGB Colors	28
4.3	Pantone Color Spectra From Yellow to Orange [27]	28
4.4	The NCS color model is based on the three pairs of elementary color [29]	29
4.5	The Adobe RGB Color Space [30]	29
4.6	RGB Color Graph [32]	30
4.7	The CbCr plane at constant luma $Y=0$	31
4.8	Four Different "Lightness" conditions [34]	33
4.9	Perceived wavelength by the human eye [35]	34
4.10	A graph of the functionality in a ROS Node [43]	37
5.1	Methodology Flowchart	40
6.1	Color Correction	46
6.2	Color Correction using CLAHE	46
6.3	Dark Channel Prior Filtering	47
6.4	LMS converted Final Images	49
6.5	ROS functionality of the process	50
7.1	UX1 Robot deployment in mine shaft with reduced visibility[11]	51
7.2	Water	52
7.3	Wall with a Structure	53
7.4	Seafloor	54
7.5	Wooden Bar from a distance	55

7.6	A Wooden Bar	56
7.7	Two wooden bars one under the other	57
7.8	A Structural beam	58
7.9	A school of fish	59
7.10	Colored fish with corals	60
7.11	Left-Original image, Right-Color corrected image from the ros node	61
7.12	Mineral Sample board	61

List of Tables

7.1	Timing-Table	62
7.2	Quality Measurement Table Original	62
7.3	Quality Measurement Table	62

**THIS PAGE
INTENTIONALLY
LEFT BLANK**

List of Abbreviations

ACE	<i>Automatic Color Enhancement</i>
ASV	<i>Autonomous Surface Vehicles</i>
AUV	<i>Autonomous Underwater Vehicles</i>
CLAHE	<i>Contrast Limited Adaptive Histogram Equalization</i>
CNN	<i>Convolutional Neural Network</i>
DCP	<i>Dark Channel Prior</i>
EME	<i>Enhancement Measure Estimation</i>
EVA	<i>Exploitation VAMOS AUV</i>
HID	<i>High Intensity Discharge</i>
HSI	<i>Hue Saturation Intensity</i>
HSL	<i>Hue Saturation Lightness/uminance</i>
HSV	<i>Hue Saturation Value</i>
ISEP	Instituto Superior de Engenharia do Porto
LMS	<i>Long Medium Short</i>
LSA	Laboratório de Sistema Autónomos
NCS	<i>Natural Color System</i>
RGB	<i>Red Green Blue</i>
ROS	<i>Robot Operating System</i>
ROV	<i>Remotely Operated Vehicle</i>
SIFT	<i>Scale Invariant Feature Transform</i>
SLS	<i>Structured Light System</i>
UCIQE	<i>Underwater Color Image Quality Evaluation</i>
UICM	<i>Underwater Image Colofulness Measure</i>
UIConM	<i>Underwater Image Contrast Measure</i>
UIQM	<i>Underwater Image Quality Measure</i>
UISM	<i>Underwater Image Sharpness Measure</i>
UUV	<i>Unmanned Underwater/Undersea Vehicle</i>

**THIS PAGE
INTENTIONALLY
LEFT BLANK**

Chapter 1

Introduction

With the increase in technology and resources from technological advancements, there are new ways to ensure human safety and progression of work in a more efficient way. From finding resources and information from around the world with the help of the internet to robots that use internet to help communicate and transfer data, the growth of technology never ceases. This has created a lot of opportunities in the field of robotics with simple robots that help clean the house, industrial robots that perform assembly, painting, welding and lots of helpful functionalities in that field, being compact and able to reach into places that are difficult or time consuming for human interaction. There is more information about the planet Mars than there is of earth and this is with respect to the water, which the earth is 70% consistent off and robotics has seen a surge in water surface vehicles, underwater vehicles and various combinations with each other and drones, remotely operated and autonomous. In underwater autonomous robotics there is now an increase in substitution of remotely operated vehicles (ROV) to an Autonomous Underwater Vehicles (AUV). All of these technological advancements have also provided an important tool, cameras and better image sensing equipment. Cameras have gotten smaller over the years with better imaging sensors inbuilt in them. The lens for the cameras gives the opportunity to gather images with a faster shutter speed and give adjustments in the focal length to see things more clearly and retain information, some can have wide angles, fixed frame and image filtering embedded in them as well. In particular the rise of robotics has driven its application into the exploration of the earth's vast water content especially underwater mines.

There exists a large a number of underwater and flooded mines that are currently abandoned with a lot of resources still available to be collected. The underwater mines are generally formed from natural causes and erosion due to water while the flooded mines can be made made with already existing structures and pathways. Depending on the depth and range of the mine there can be a lot of environmental changes, from light, the materials in the water, living organisms, radioactive properties and man made structures in the case of flooded mines. This poses a vast variety of challenges for people to go into to collect

and gather resources, samples and images. Underwater robots provide a step in the right direction of the solution to be able to obtain more information.

This thesis describes the image cleaning and enhancement of images in underwater scenarios, mainly the mining application in robotics. It is oriented to two main purposes, better human visualization and automatic processes for the robot to navigate and collect data. It is based on two of the methodologies, performing colour correction on images, performing Dark Channel Prior (DCP) to the corrected images and then taking the final modified images and converting them into the Long Medium Short (LMS) color space, as this space is the region in which the human eye perceives colour.

This dissertation was developed in the context of the Master's Degree in Electrical and Computer Engineering carried out at the Laboratório de Sistemas Autónomos (LSA) of the Instituto Superior de Engenharia do Porto (School of Engineering of Polytechnico Porto, ISEP).

As ocean exploration increased, the area of underwater image processing has drawn more and more attention over the last years, since video and image are the important ways to obtain and record information nowadays, and the implementation of video and image processing becomes more and more wide.

The visual quality of underwater images has a decisive and critical role in many ocean engineering applications and scientific researches, such as marine ecological research [1], monitoring sea life [2], taking census of populations, ocean rescue, repair of structural damage and assessing geological or biological environments like coral reefs [3].

Underwater imaging is challenging due to the physical attributes existing in such environments. Unlike normal images, which are taken on the surface, underwater images suffer from poor visibility due to the attenuation of the propagated light [4]. The light is attenuated exponentially with the distance and depth mainly due to absorption and scattering effects. The absorption substantially reduces the light energy while the scattering causes changes in the light direction. There is also a random attenuation of light which is the main cause of the foggy occurrence. The fraction of the light scattered back degrades the scene contrast and this causes a contaminated image with the color. This is one of the reasons why underwater images usually have a tinge of blue or green the deeper the distance underwater, in some cases brown due to the mud, and objects at a distance seem foggy.

These effects aren't only a result of water but also the addition of other components such as dissolved organic matter or small floating particles. External lighting fixtures can be added to capture a better image with more context in the frame. In some cases, the artificial light can even effect the image in a bad way due to excessive lighting, non-uniform dispersion of light, camera being too close to the light source and light with particles surrounding it. Fundamentally, in common sea water, the objects at a distance of more than 10 meters, on the account of the colors that are fading where the characteristic wavelengths

of light are cut according to the water depth, seem indifferent. Image enhancement for underwater applications such as mining would improve navigation, quality and precision.

An AUV also known as Unmanned Underwater/Undersea Vehicles (UUV) is a robot that travels underwater without requiring input from an operator with a very distinct set of applications. From the scientific point of view, AUVs can provide support in the mapping and reconstruction of ocean soil [5], establishment of communication between different vehicles of it's own class or subclass and also with an Autonomous Surface Vehicles (ASV), and data acquisition for eco-systems studies.

From the military point of view, monitoring of ports and coastal regions for recon missions, payload delivery, Oceanography and ocean patrol for surveillance and mine counter-measures can be carried out by an AUV. It can also be helpful in rescue missions. AUVs can also provide support in the exploration and maintenance of oil pipelines, oil rigs and underwater mining in a cost effective manner with minimum disruption to the environment. In scenarios of natural disasters where humans cannot reach due to radiation or any other circumstance, AUVs can easily explore and inspect the site. AUVs are also very important in Air-crash Investigations and finding ships which are lost in sea.

The motivation behind this topic is not only to identify and create a solution for mining, but also provide a better image processing of underwater images for robotic applications such as feature extraction, detection of minerals and life forms, and structural damages. Cleaning and enhancing the underwater images provides them to be visibly pleasing to the eyes with a better contrast and to be able to extract more information from the original. This can be directly used by humans for a better visual context of the images or the robots by an automatic processing image algorithm.

1.1 Objectives

The main objective of the project, is to develop a real time algorithmic solution to clean and enhance underwater images to be able to extract more information and make it visibly clearer for the application of underwater mining. To meet this end, the following objectives must be met:

- Study of existing image processing techniques and methodologies
- Examine and Identify the problem to solve
- Develop an Image Enhancement solution with the main focus in mining
- Collect Data-sets from the real world mine explorations
- Implementation for the color correction in real time
- Testing the method

- Validation and Characterization of the images with a grading metric
- Testing and validating the project in real scenarios

1.2 Thesis Structure

This thesis is organised as follows: After the introductory chapter it is followed by a problem analysis and formulation which is addressed in Chapter 2. The current State Of The Art in image enhancement for underwater scenarios is presented in Chapter 3. Relevant theoretical background concepts are presented in Chapter 4. The proposed solution is presented in Chapter 5 with the implementation details described in Chapter 6. Finally results are presented and discussed in Chapter 7 along with some concluding remarks and future work that are presented in the last Chapter.

Chapter 2

Problem Formulation

In Europe, it is estimated that there are around 30,000 closed mine sites. Many of these still may have considerable amounts of essential raw materials. However, most of these closed mines are now flooded and the last piece of information of their status and layout is decades or more than a hundred years old. The complex underground layout, topology and geometry of most underground mines, make it impossible to do any surveying by conventional or remotely controlled equipment.

With the increase in technology and resources from technological advancements, there are new ways and faster methods to solve problems underwater without the danger and putting lives at risk of highly skilled divers. In autonomous robotics there is now an increase in substitution of remotely operated vehicles (ROV) to an AUV. Either it be for exploration or retrieving samples, now robots are able to do it in a faster time with less human danger while carrying a lot of advantages. Robotic exploration for underwater caves, closed spaces, abandoned shafts and underground mines pose a new and difficult problem. With this poses the treat of the size of the robot to be able to explore the mines. Robots need some guidance or guides for them to be able to see and navigate underwater.

Each Robot can have a different set of configurations, from the processing unit, camera, light fixture, mobility and control. The robot will need a lot of information for it to be able to understand its surroundings. The fastest response is through sight which is from the cameras that help the robot see what is in the surroundings. The camera alone cannot help the robot under a certain depth as light propagation comes into effect as seen in chapter 4.

Robots are built with these imaging phenomenons in mind, that there will be loss of clarity in vision the deeper it has to travel. Lighting fixtures help resolve this problem, but each robot has its own implementation of the lighting fixture.

The problems have motivated the creation of projects like VAMOS! and UNEXMIN which are mainly oriented to researching, exploring and extracting mines. The project VAMOS! [6] which aims to create a robotic systems solution for the exploitation of flooded open pit mines, submerged, deeper-seated minerals to be able to mine those unreachable

mineral deposits in a safe, environmental friendly and economically sustainable way. The VAMOS! project deals with open mines, inland mines and shallow waters. The depth of the mine can vary from the locations of the mine sites but since it is shallow water and open pitted mines it is close to 0-50m underwater with natural light present. It also depends on the the mineral ore being mined, as clay cause a very mucky visible condition while as quartz is clear.

The Mining Machine as seen in figure 2.1 is a mining machine that has blades that mine the ore, a front facing camera, studies the deposits, and EVA (Exploration VAMOS AUV) [7] was built to support, as a hybrid ROV/AUV for the VAMOS! project. Eva, which is an innovative development for operations support in inland underwater mining operations. This robot can be used in a wireless ROV tele-operation mode and in autonomous AUV mode. The robot was developed for the project VAMOS! which was created with a vision based system which comprises of a custom Structured Light System (SLS) [8] which was developed by INESC TEC which is composed of a smart camera with embedded processing and a light projector. The vehicle uses two SLS at the front in order to extend the coverage area and a downward looking one for bottom coverage as seen in figure 2.2. It is used for real-time pit modelling and for assisting the underwater cutting operations providing visual and detailed sonar information from multiple points of view of the cutting, launch and recovery of the miner robot. In a challenging environment, such as the underwater mining scenario, in industrial conditions, providing crucial data for the planning, supervision, command and control of the mining system.

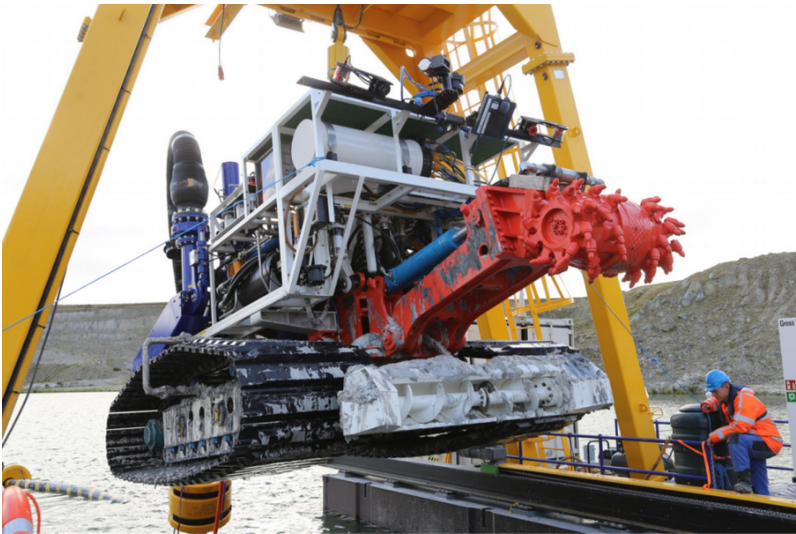


Figure 2.1: Mining Machine

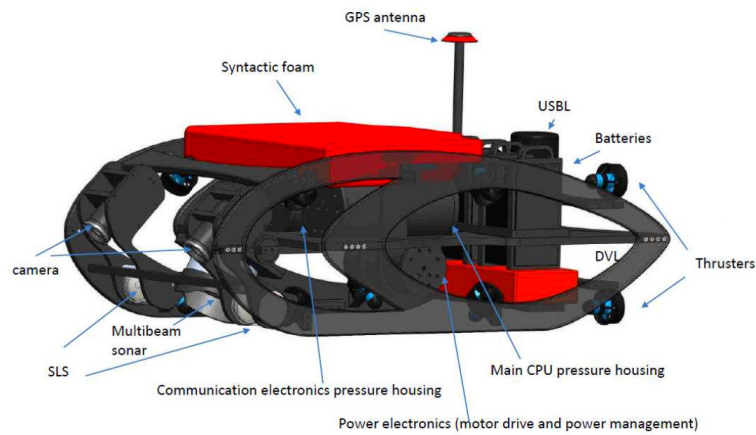


Figure 2.2: Model of EVA [7]



Figure 2.3: Deployment of EVA at Lee Moor Mine, UK

Recently, smaller size underwater robots such as the SPARUS UUV have been used in the characterization of marine underwater caves [9] which uses two optical vision systems, one is a forward and down looking analog camera and the other is a GoPro Hero2 3D. It uses a lighting system of 2x24W High Intensity Discharge (HID) lights. Its main purpose is to collect imagery of the ocean cave floor and reconstruct a 3D shape of the cave with the help of other sensors.

The UNEXMIN projects [10], which is aimed to develop new technologies for exploration and 3D mine mapping of flooded underground mines and deep mines by developing a fully autonomous multi-platform Robotic Explorer. Underground mines have shafts and structures which pose a problem, an additional problem is the tight space which make it

extremely difficult for even the most skilled divers to go into. Each mining scenario is different, some require multiple exploration missions which can provide a wide data for analysis and understanding the environment because of the unfavourable conditions that it can pose. The data obtained can be used to produce a computational understanding of the mine as well. Based on the collected data and the vast amount of data extracted it will be useful information for understanding the scene that the robot is in and the actions it needs to perform if any. The waters are also very different depending on the mine as some can have clear waters, some murky water, some with current inside it.

Different mines pose different properties and difficulties, like for example in Urgeiriça which was a test site of UNEXMIN located in Portugal, was the biggest uranium producer in Europe, the mine contains a lot of minerals like magnetite or pyrrhotite and metallic objects left behind in the abandoned mines which cause the water to be a murky brown color. As the maximum depth of the mine is 450m, the water thickness is changing from point to point, the water color can be different, also depending on the clarity of the water the number of particles that can exist in one frame can increase or decrease. The number of particles in the area can also be influenced from the motor of the robot which can be circulating the particles back into the same area. The robot is also facing conditions of high pressure and acidic water.

The Kaatjala mine in Finland is a open large lake with mine structures and shallow water. Kaatjala, known for its big pegmatitic deposits, once hosted big mining quartz and feldspar operations in the past. The main rock types of the area are gneisses and mica schists of sedimentic origin. The mine ranges a maximum 30m in depth and 620m in length.

The Idrija mine in Slovenia is now considered as an UNESCO Heritage site – this made it vital that the UNEXMIN technology could work as a non-damaging, non-contact as the mine cannot be damaged in any way. The mines main resource is mercury which in total, around 700km of tunnels and shafts reaching 380 metres in depth at 15 different levels were excavated during its lifetime. Idrija mine has a lot of shafts and horizontal submerged tunnels, although currently most of them are back-filled.

Ecton mine, United Kingdom, has a main resource of copper with important quantities of lead and zinc. The mine was active from the 1500BC to 1880AD. The minerals were found as a "pipe vein" or vertical vein 310m below river level.

Compact robots like the UX-1 [11] which was developed for the UNEXMIN project, is built with a smaller size which has its equipments and lighting fixtures in its compact spherical shape. The cameras are placed next to the light fixture as seen in figure 2.4, the robot has five digital cameras and a main light and laser source.

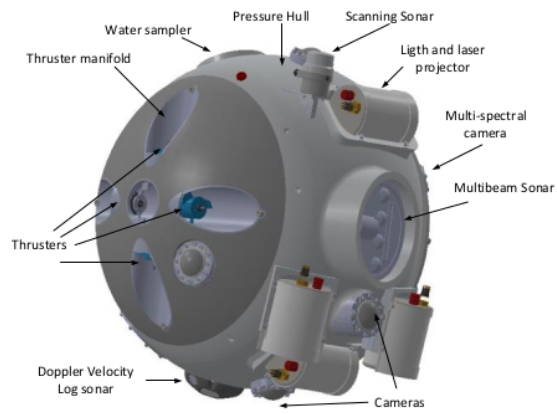


Figure 2.4: Model of UX-1 [11]

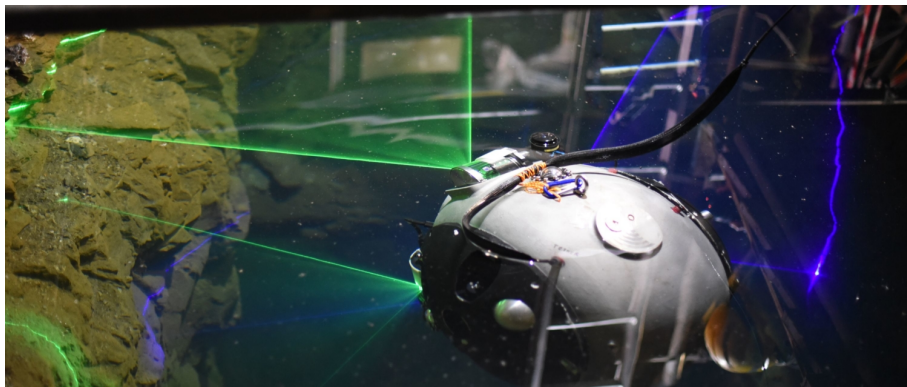


Figure 2.5: UX-1 entering the Ecton mine, UK



Figure 2.6: UX-1 exploring Ecton mine

A real image taken of a mineral sample board from the camera closer to the light source, the multi-spectral camera, in the environment of a mine can be seen in the figure 2.7, where the robot is relatively close for it receive good information about the surrounding.

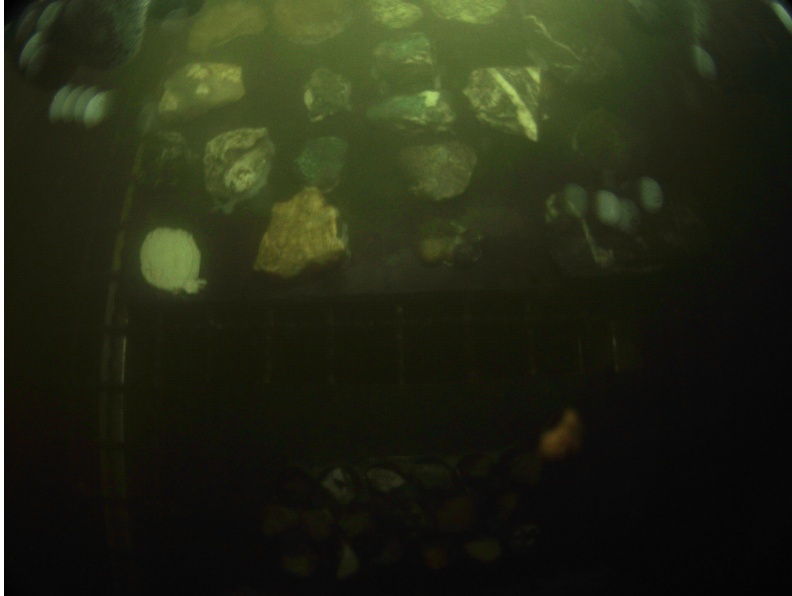


Figure 2.7: Mineral sample board placed in Idrija Mine

This brings up problems with imaging like color absorption which is an effect due the wavelength of light passing through the water and objects which also brings into effect the physical properties of reflection and refraction.

We also identify the problems from illumination and lighting effects, color degradation and reflective details from the foggy effect that comes onto the images.

Problems arise with more depth as the color of the water starts to get a deeper shades of blue and green due to the light properties. There is also an environmental factor where water in mines can be contaminated by the dissipation of minerals over time. There can also be fishes and dirt particles that are floating which can act as an interference in the view of the camera.

There is also the factors of poor quality and loss of features and information from various sources that should be taken into consideration.

Chapter 3

Related Work

A significant amount of work in Image Enhancement has already been done by using various techniques.

Iqbal [12] proposes a method based on slide stretching using an integrated color model. First, contrast stretching is done with the RGB algorithm to equalize the color contrast in the image. Then a saturation and intensity stretching of (Hue, Saturation, Intensity) HSI color space is done to increase the true color and resolve the lighting problem. Using the HSI model, there is control over contrast modifications in the image with the S and I values. The contrast stretching algorithm is applied to each channel so the scaling and color ratio is maintained.

Kaur [13] proposes a comprehensive algorithmic technique, where preprocessing is done to the image and calculation of image size. They then proceed to convert the image from RGB into LAB color space to implement Contrast Limited Adaptive Histogram Equalization (CLAHE) and modify the light component. The image is converted back into RGB from LAB and a gradient based smoothing is applied. This work is a standard conceptualization of image enhancement for underwater images.

Another approach is done by performing the color correction under the Ruderman opponent colour space $l\alpha\beta$ as explained by Bianco [14] in their methodology. Here, the l is the luminance component and α and β are the color components. One encodes yellow-blue and the other red-green chromatic. This method uses histogram stretching and luminosity cutoff, where the image undergoes changes from a non-linear RGB colour coordinates to the $l\alpha\beta$ colour coordinates. This is achieved by taking the gray world and uniform illuminations and expressing them in a RGB color space which is modified into an LMS color space. Those corrected states of coordinates are brought back to a RGB color space which are then converted into the $l\alpha\beta$ color space with a white point correction as a result.

Zhang [15], uses a two step combination of colour correction and illumination adjustment. The colour correction method calculates the mean value and the variance value among the three channels, independently and the maximum and minimum values are taken

and normalized to get the corrected value. The illumination adjustment is done on the (Hue, Saturation, Value) HSV space and based on the Retinex model [16], the illumination component is estimated and corrected. The image is color corrected in the RGB space and then converted to HSV space to modify the values on the V layer. The energy is decomposed in the Value layer and gives two components, Reflectance and Illumination. The illumination component is assumed, from which the reflectance component is obtained and solves the issue of under-exposure.

Park [17] uses gradient compensation to improve the color contrast and clears color distortion. The method is comprised of three steps, the first, taking the RGB image and converting it into gradient domain. This causes some information loss. The second, the degraded magnitude of gradient is compensated with the transmission map estimate. This adopts a distance estimation method which removes the problems of low contrast and blurring. The last, returning the image back to RGB with a novel boundary condition. This rectifies the color change problem.

Hitam [18] proposes a new method called Mixture Contrast Limited Adaptive Histogram Equalization (CLAHE-MIX) color models that is developed for underwater image enhancement. The method operates CLAHE on RGB and HSV color models and combines both results together. The main goal is to reduce the noise produced on the images by using the method of CLAHE. The CLAHE-MIX normalizes the CLAHE from the RGB space, converts the CLAHE HSV space to RGB and added with a normalization.

Li [19] describes a hybrid image correction method. This includes color correction and image dehazing. They also estimate a global background light and medium transmission to the three channels.

Ancuti [20] uses fusion principles to enhance underwater images and video. This framework uses specific inputs and weights to overcome limitations in the environment. The first derived input in the single-based image approach is considered as the color corrected image and the second is considered to the contrast enhanced one after noise reduction is performed. A white balancing is done to the inputs and then a noise correction is performed. A linear and non-linear filter is used to smooth the results.

He [21], Single Image Haze Removal using Dark Channel Prior (DCP) uses the dark channel prior to remove haze in an image which is essential for underwater image enhancement techniques. Haze remove increases the visibility of the scene and improves information for vision algorithms and further editing. Dark pixels can directly provide accurate estimation of the haze's transmission in an image. Recovering the scene radiance and the estimation of the atmospheric light provides a clear dehazed image.

Sathya [22], incorporates DCP into underwater image enhancement. Sathya's methodology extracts the colour features and source of illumination, performs a dark channel estimation and then removes the haze from the image. Ancuti [23] uses a locally adaptive colour correction with a model DCP with colour shifts in their fusion technique which is

mentioned above and rectifies colour changes in the intensity. Various Illumination properties have been added. Reference images help solve the color correction better. The reference images used can be an original image taken out of water or the original image which is over layed onto the enhanced image to keep some features. The usage of color channels are a part of the illumination process in this methodology. Scale Invariant Feature Transform or SIFT is a feature detection algorithm in computer vision to detect and describe local features in images and it used for matchmaking for features to give a better understanding of the result.

Deep underwater image enhancement using a Convolutional Neural Network [24] has a trained database which generates enhanced images. The training set uses the attenuation coefficients from [25] for different ocean and coastal waters. A set of synthetic underwater images, normal pictures with added effects simulating underwater images, were used to test and calibrate the system for clear images. 10 types of underwater image sets were built with 1449 images out of which 1000 images were used for training and 449 images were used for validation. The input images were taken in the size of 310x230 and applied to a model using ADAM [26], which is an algorithm for first-order gradient-based optimization method, on Tensorflow, which is deep learning framework, with the batch size set to 16. Once, the value is quantified it is applied to real underwater images. These images are then post processed in the HSI space to improve the saturation, contrast and brightness of the image.

**THIS PAGE
INTENTIONALLY
LEFT BLANK**

Chapter 4

Theoretical Background

4.1 Light Properties

White light is distributed into the rainbow colors of the visible spectrum of Red, Orange, Yellow, Green, Blue, Indigo and Violet. White light is the combination of different frequencies of visible light that are a part of the visible spectrum.

When light hits the water surface, there are some phenomenon that happen, such as, reflection, transmission, refraction and absorption. The light that is refracted into water can be absorbed by living or non-living entities which gives those bodies their color, which is the selective absorption of light waves. Objects that reflects all the frequencies from the spectrum appear to be white, while objects the absorb all the frequencies appear black.

In water the dispersion of those frequencies degrade over depth and light with shorter wavelengths pass through as seen in figure 4.1 causing only certain frequencies of light to pass through after certain depths. The further we travel underwater the prominent the frequency of the blue color is.

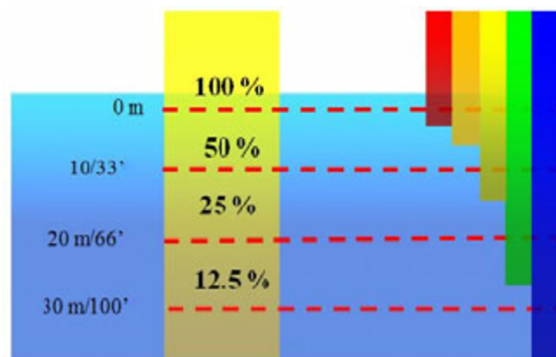


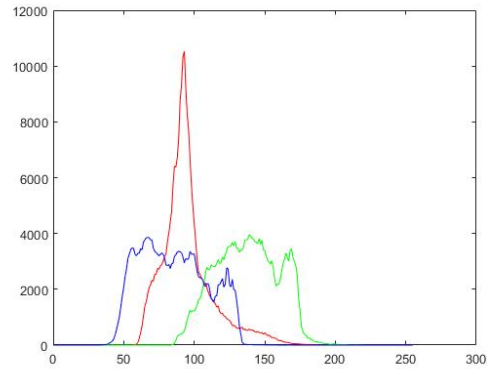
Figure 4.1: Dispersion of light underwater

4.2 Color Spaces

The light properties allow the blue and green color travel longer in the water due to their shorter wavelength and this causes underwater images to be dominated by a blue or green color. When a histogram is plotted on any underwater images the distribution ranges of three channels usually does not cover the entire range [0,255] considering a single pixel value representation as seen in figure 4.2b.



(a) Fishes with Coral



(b) Histogram Value of the Image

Figure 4.2: Histogram Graph of the RGB Colors

Color Spaces are a palette of colors which range from different spectrum's in a specific organisation. There are a few standard collections like Pantone collection, and systems like NCS system and Adobe RGB system. The Pantone collection has a system called Pantone color matching system which is a largely standardised color reproduction system for industries and pigmentation. Applications include inks, wall paints, nail color, and beauty products. This follows the CYMK which is Cyan, Magenta, Yellow and black, which was used for printing and is a color module. Example color spectra in figure 4.3.

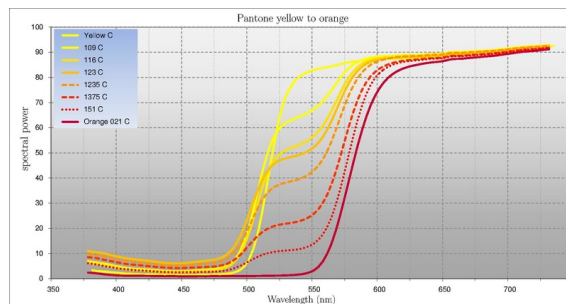


Figure 4.3: Pantone Color Spectra From Yellow to Orange [27]

The NCS system is known as the Natural Color System, is based on the color opponency hypothesis of color vision, first proposed by German physiologist Ewald Hering [28]. It

states that there are six elementary colors, white,black,red,yellow,green and blue as seen in figure 4.4.

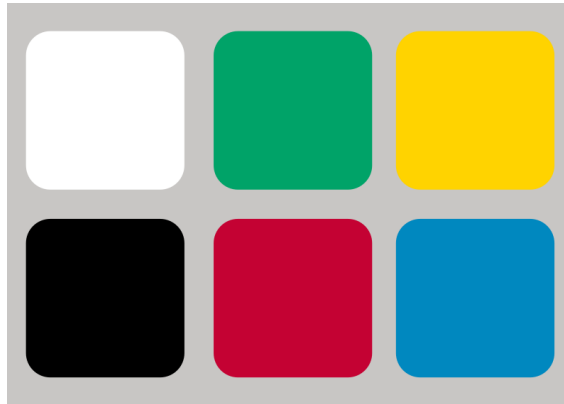


Figure 4.4: The NCS color model is based on the three pairs of elementary color [29]

The Adobe RGB color space was developed in 1998 and is primarily used for color displays using RGB as the primary colors to encompass the color scale set by the NCS system. Breaking this down it was found there exists completely different color spaces based on the same RGB color model. This brought a reference standard which is the CIELAB or CIEXYZ color spaces that encompass the color ranges that is perceived by the human eye, seen below in figure 4.5.

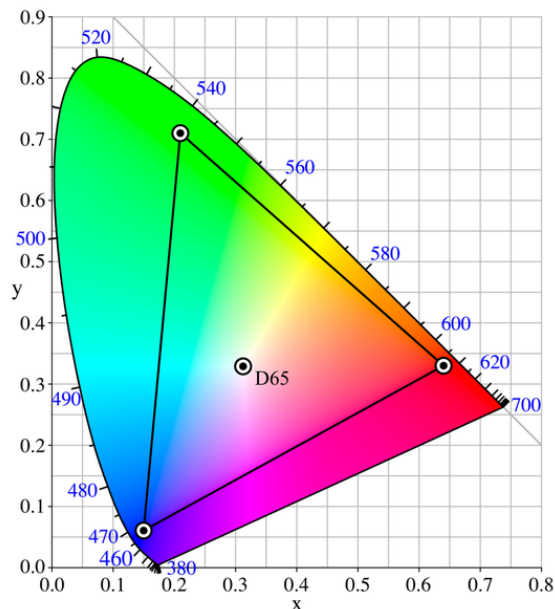


Figure 4.5: The Adobe RGB Color Space [30]

Hence "color space" can identify as a particular combination of the color model and the

mapping function, but is often used informally to identify a color model. Several specific color spaces are based on the RGB color model but there is no such thing as the singular RGB color space. The color space is usually defined as a channel having 256 levels, this means that for 3 channels, $256 \times 256 \times 256$, there is an approximate 16.7 million color ranges.

The list of color spaces that exist are function based, they originate from the different color modules [31]. The RGB (Red, Green and Blue) is a color module as well as a color space which is an additive color space based on its color model. It is a definition of the three primary colors and a white point in the center as in figure 4.6.

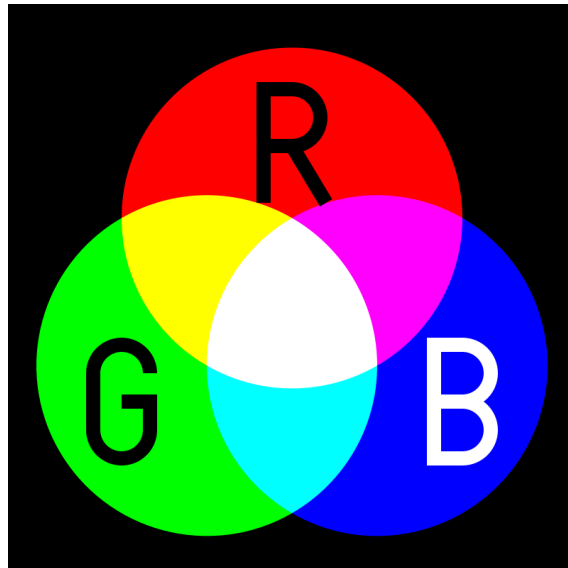
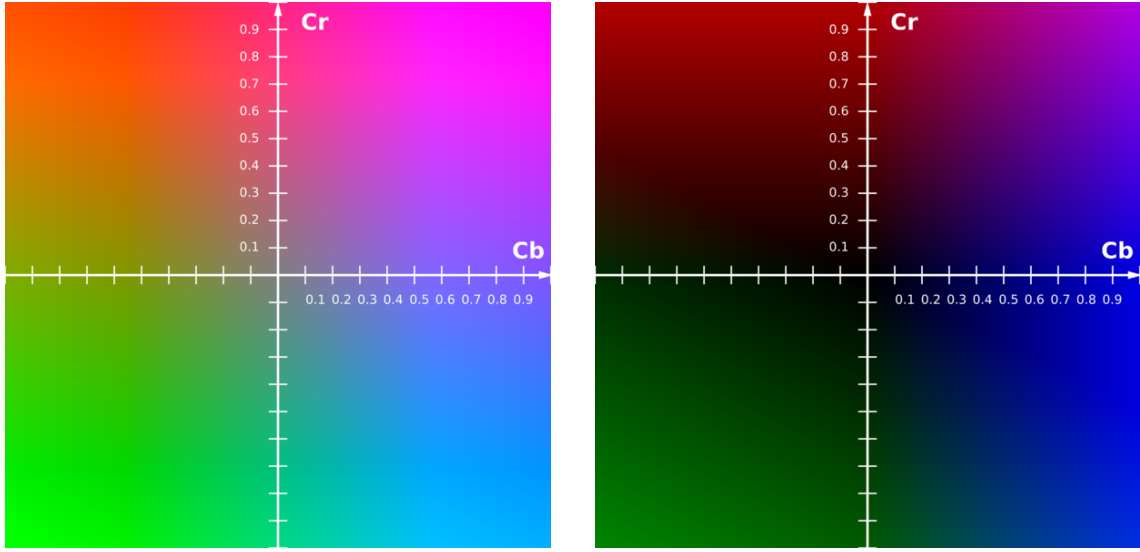


Figure 4.6: RGB Color Graph [32]

The color lists that belong to Luma plus chroma were mainly developed for the television/screens and jpeg conversions. The luma stores the value of the chroma/chrominance which is the signal used to convey the color information on to the screen. The most commonly used color list is the YCbCr which has optimized high dynamic range as its main application is in video and image compression. The Y stands for the luma component, Cb, the blue-difference and Cr the red-difference in chroma points.



(a) The CbCr plane at constant luma $Y=0.5$

(b) The CbCr plane at constant luma $Y=0$

Figure 4.7: The CbCr plane at constant luma $Y=0$

YCbCr signals are created from the corresponding gamma-adjusted RGB source using three defined constants K_R , K_G and K_B :

$$\begin{aligned}
 Y' &= K_R \cdot R' + K_G \cdot G' + K_B \cdot B' \\
 P_B &= \frac{1}{2} \cdot \frac{B' - Y'}{1 - K_B} \\
 P_R &= \frac{1}{2} \cdot \frac{R' - Y'}{1 - K_R}
 \end{aligned} \tag{4.1}$$

where K_R , K_G , and K_B are ordinarily derived from the definition of the corresponding RGB space, where $K_R + K_G + K_B = 1$. Depending on the luma Y the intensity changes of K_R , K_G and K_B as seen in figure 4.7.

There is a list of cylindrical transformation which is the HSL and HSV spaces that are defined as mappings of RGB. They are defined as the Hue, Saturation and Value (HSV) and Hue, Saturation and Lightness/Luminance (HSL) with the underlining difference is that in HSL a light color appears white, whereas in HSV the color appears brighter or darker depending on the light.

Hue is defined as the attribute to associate the area in a image to one of the perceived colors or combination of two of them [33]. Saturation is the "colorfulness of a stimulus relative to its own brightness" [33]. Lightness is the "brightness relative to the brightness of a similarly illuminated white" [33]. Brightness and Colorfulness is absolute measures, while lightness and chroma are related to some white point in the space.

Hue mathematically is defined as the ratio between the maximum value of the R,G,B chroma minus the minimum value of the R,G,B chroma. Let us define C as the chroma

value:

$$\begin{aligned}m &= \text{Min}(R, G, B) \\M &= \text{Max}(R, G, B) \\C &= M - m\end{aligned}\tag{4.2}$$

So Hue is the proportion of the distance around the edge of the hexagon which passes through the projected point, originally measured on the range $[0, 1]$ but usually measured in degrees $[0, 360]$ which translates to:

$$H' = \begin{cases} \text{undefined,} & \text{if } C = 0 \\ \frac{G-B}{C} \bmod 6, & \text{if } M = R \\ \frac{B-R}{C} + 2, & \text{if } M = G \\ \frac{R-G}{C} + 4, & \text{if } M = B \end{cases}\tag{4.3}$$
$$H = 60^\circ \times H'$$

The simplest definition for Lightness is just the average of the three components R,G,B in the HSI model called intensity, in the HSV model it is the largest component of a color and HSL model it is the average of the largest and smallest color components.

$$\begin{aligned}I &= \frac{1}{3}(R + G + B) \\V &= M \\L &= \frac{1}{2}(M + m)\end{aligned}\tag{4.4}$$

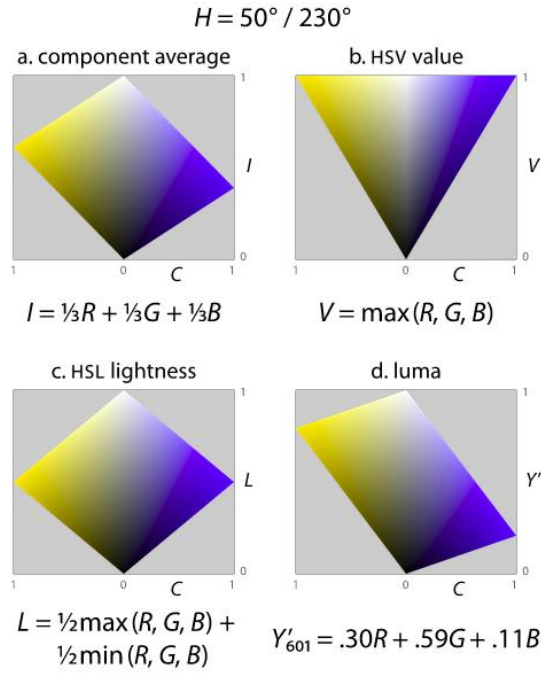


Figure 4.8: Four Different "Lightness" conditions [34]

Saturation is when the HSL and HSV models scale the chroma so that it always fits into the range $[0, 1]$ for every combination of hue and lightness or value. It can be written mathematically as:

$$\begin{aligned}
 S_{HSV} &= \begin{cases} 0, & \text{if } V = 0 \\ \frac{C}{V}, & \text{otherwise} \end{cases} \\
 S_{HSL} &= \begin{cases} 0, & \text{if } L = 1 \vee L = 0 \\ \frac{C}{1-|2L-1|}, & \text{otherwise} \end{cases}
 \end{aligned} \tag{4.5}$$

The XYZ color space is absolute color space which is the opposite of a generic color space like RGB. It is a Tristimulus value that appeals to all the wavelengths the human can perceive. The model captures the Y as the luminance, X is a mixture of response curves that are chosen to be non-negative and Z as a quasi-equal to blue. It works in conjunction with LMS.

LMS is classified as a special case color space represented by the response of the three types of cones of the human eye, named for their responsivity (sensitivity) peaks at Long, Medium, and Short wavelengths.

There are many transition matrices that can be used to translate the XYZ to LMS,

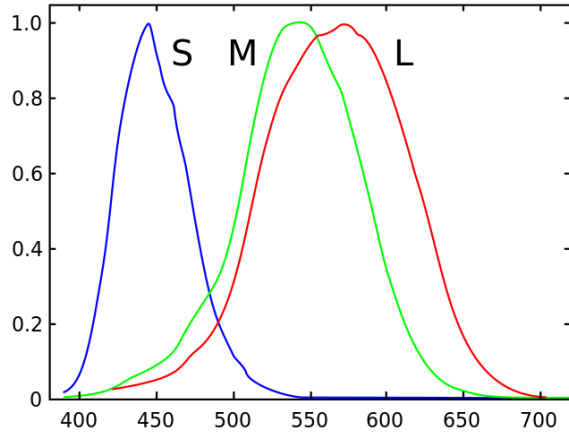


Figure 4.9: Perceived wavelength by the human eye [35]

such as normalized to D65

$$\begin{bmatrix} L \\ M \\ S \end{bmatrix} = \begin{bmatrix} 0.4002 & 0.7076 & -0.0808 \\ -0.2263 & 1.1653 & 0.0457 \\ 0.0000 & 0.0000 & 0.9128 \end{bmatrix} \begin{bmatrix} X \\ Y \\ Z \end{bmatrix} \quad (4.6)$$

which is to represent average daylight and a temperature related color correction to the image.

Mark Fairchild [33] states another approach using the LLAB color model and CIECAM97 color appearances to create a transition matrix which was then a revised CIECAM97 [36] being a useful standard and CIECAM02, which is the successor to CIECAM97, which is a "spectrally sharpened" transition matrix as it has narrower response curves which make the cones more distinct [37], it can be formulated as

$$\begin{bmatrix} L \\ M \\ S \end{bmatrix} = \begin{bmatrix} 0.8562 & 0.3372 & -0.1934 \\ -0.8360 & 1.8327 & 0.0033 \\ 0.037 & -0.0469 & 1.0112 \end{bmatrix} \begin{bmatrix} X \\ Y \\ Z \end{bmatrix} \quad (4.7)$$

and for CIECAM02

$$\begin{bmatrix} L \\ M \\ S \end{bmatrix} = \begin{bmatrix} 0.7382 & 0.4296 & -0.1624 \\ -0.7036 & 1.6975 & 0.0061 \\ 0.0030 & 0.0136 & 0.9834 \end{bmatrix} \begin{bmatrix} X \\ Y \\ Z \end{bmatrix} \quad (4.8)$$

4.3 Formation of Images

The imaging process is a mapping of an object to an image plane. Each point on the image corresponds to a point on the object. A grayscale image is where the value of each pixel is a single sample representing only an amount of light, the intensity information.

Grayscale images are composed only with shades of gray and contrast from black to white, where 0 is total black and 1 is white. A color picture frame is divided into rows and columns, each block has a pixel. This pixel contains 3 channels which are Red, Green and Blue respectively. We distribute those 3 channels as their own respective channel and find out the intensity in that pixel, where the range is from 0 to 255.

4.4 Normalization

Normalization is an image processing method that changes the range of pixel intensity values which is within the spectrum of 0 to 255. This helps with reduction of poor contrast due to glare, or not enough lighting in the surrounding area. Normalization is sometimes called contrast stretching or histogram stretching which resolves and can modify each pixel. Normalization was first implemented on black and white and grayscale images to provide more detail in the images, now it is widely implemented in color images to achieve the same effects.

In normalization the image size is taken and the pixels are split into their respective rows and columns. The image can be converted into any color space or grayscale, as the normalization methodology works on the illumination values in the pixels.

$$I_{new} = (I - \min_{r,g,b}) * \frac{255}{\max - \min} \quad (4.9)$$

There are several other methodologies that can follow the same principles, such as Automatic Color Enhancement (ACE) [38] where it amplifies small differences and saturates large differences. This helps the entire image to gain a global white balance. In the usage of Simplest Color Balance [39], an affine transform is used of the form $ax+b$ to each channel, computing a and b so that the maximal value in the channel becomes 255 and the minimal value 0. Although this may not result in an improved image, it improves it's overall understanding of the image content.

The pixels distributed into the 3 channels as their own respective channel, the intensity can be find out for each pixel. Obtaining its neighbouring pixel value and comparing it with the previous one to see if the intensity is greater or not. If it is less than the previous one we bring it up to the same value as the previous one, if it is greater than the value we bring it down to the previous. This methodology is known as the nearest neighbour [40].

4.5 Dark Channel Prior

The Dark Channel Prior is based on the statistics of obtaining haze-free images. "Dark pixels" are pixels with low intensity in at least one RGB color channel. In a hazy image, the intensity the dark pixels in any channel is mainly contributed by the airlight, which is

the ambient light reflected into the line of sight by atmospheric particles [41]. These dark pixels can directly provide accurate estimation of the haze's transmission.

Normal dehazing method: Find Intensity using J and A which is scene radiance and atmospheric light and t is the medium transmission of light [42].

$$I(x) = J(x)t(x) + A(1 - t(x)) \quad (4.10)$$

In DCP the values found are J_{dark} and $J_{\text{dark}}(x)$ for an image I which is the DCP component.

$$J^{\text{dark}}(\mathbf{x}) = \min_{\mathbf{y} \in \Omega(x)} \left(\min_{c \in \{r, g, b\}} J^c(\mathbf{y}) \right) \quad (4.11)$$

where J^c is a color channel of J and $\Omega(x)$ is a local patch centered at x . Due to the additive airlight, a haze image seems to be brighter than its haze-free version in where the transmission t is low. So denser regions have higher intensities.

Estimating the Transmission \tilde{t} : Atmospheric light, A is assumed. Here we find out the patch transmission, where ω is a constant parameter ($0 < \omega < 1$) which is set at 0.95, which can simplified as:

$$\tilde{t}(\mathbf{x}) = 1 - \omega \min_{\mathbf{y} \in \Omega(\mathbf{x})} \left(\min_c \frac{I^c(\mathbf{y})}{A^c} \right) \quad (4.12)$$

Scene Radiance: With the atmospheric light and the transmission map, we can recover the scene radiance. The direct relation can be very close to zero when the transmission $t(x)$ is close to zero. The scene radiance can $J(x)$ is:

$$\mathbf{J}(\mathbf{x}) = \frac{\mathbf{I}(\mathbf{x}) - \mathbf{A}}{\max(t(\mathbf{x}), t_0)} + \mathbf{A} \quad (4.13)$$

4.6 Robot Operating System

ROS (Robot Operating System) is a framework and software library created to standardize the way of communicating in robotics. It is an open-source, based on message-based and tool-based. ROS uses a system of libraries designed to be used independently that is comprised of a set of nodes representing processes that communicate across systems using messages. The information produced in the nodes may be subscribed, if you want to access the information contained in the node, or published, if you want to save information to be subscribed to by other nodes of ROS, as seen in figure 4.10.

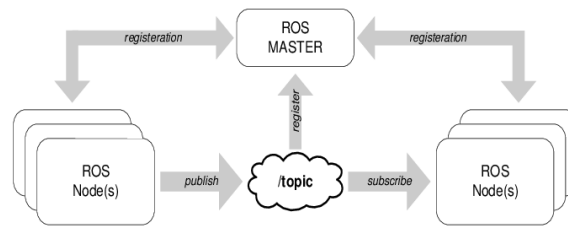


Figure 4.10: A graph of the functionality in a ROS Node [43]

Messages are organized by topics, topics are the descriptions of the messages that are used in a subscriber and publisher. The messages are processed by using the publisher-subscriber model. Messages are passed by peer to peer communication and do not have to be written in any specific programming language, since nodes can be written in C, C++, python, LISP, Octave or any language provided for ROS. ROS runs on linux only and the ROS philosophy is inspired by Unix's: Tools designed to communicate with each other in an environment open to any programmer.

ROS's libraries and nodes are organized into packages that contain the definitions of the messages the package can use. Each package must have features enough to be useful as packet. The ROS system inputs are given from the user defined nodes which also has a central master (roscore) responsible for the initial communication establishment with the central network for transfer of information [44].

**THIS PAGE
INTENTIONALLY
LEFT BLANK**

Chapter 5

Design Solution

Image Enhancement is a crucial part for any image correction regarding underwater. Visual quality helps identify objects, living organisms and even materials. As the Underwater Robotics applications have grown various methodologies for image enhancement and clarity underwater have been made.

The proposal of the methodology follows the corresponding steps, the initial being color correction of the image by performing a contrast stretch and equalization to each pixel in the image on the all channels, that is Red, Green and Blue respectively. The image is still foggy and unclear after this, so dehazing the image using DCP is done next. Once the image has been dehazed we perform a conversion to the LMS color space as it is the representative color space that the human eye perceives color.

Our main goal is to develop a methodology for cleaning and enhancing images that have been captured in underwater mining scenarios for better vision, the detection of minerals and structures and to be able to integrate this algorithm and provide a real time solution or effective enough solution for autonomous underwater robots. Thus, the improvement of image contrast, cleaning and enhancement are investigated since we can use that information for other aspects like feature detection or navigation and those techniques can access this information and be operated independently.

A diagram of the proposed method is shown in figure 5.1. The process is broken down as follows: First, a color correction is done to solve the color cast, second, we apply DCP to the color corrected image and solve the hazing problem, lastly, we convert the image to XYZ, then convert it from XYZ to LMS. In some cases a simple color balance can be added to make the image more visually pleasing.

5.1 Color Correction

To solve this problem, a color correction method is implemented which calculates the mean value among the three channels, independently. The values along each channel have

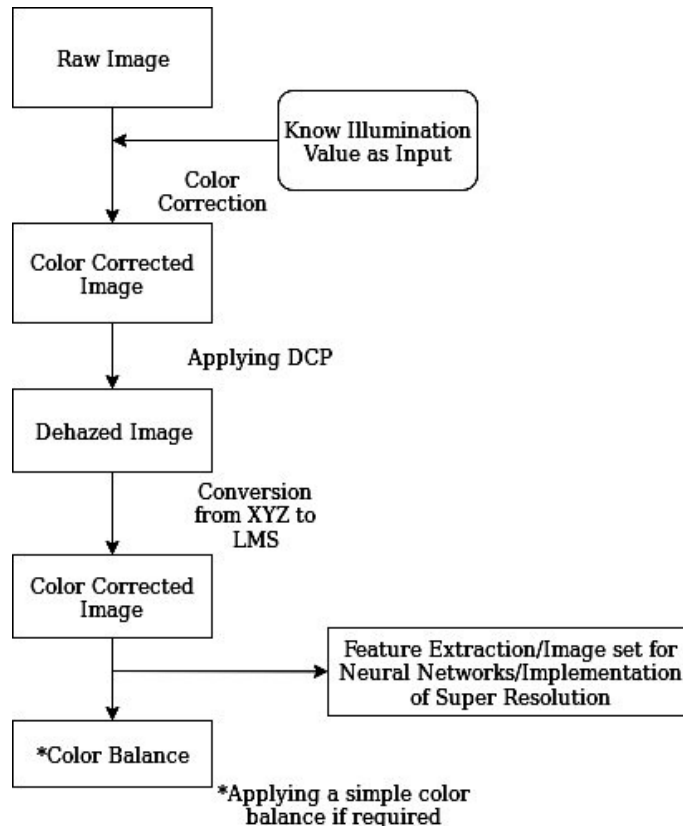


Figure 5.1: Methodology Flowchart

a constant value to help equalize the colors. After the minimum and maximum values are found, the values are used for normalization which gives an even and average histogram distribution range to all the channels.

For our methodology, we first find the mean values of the pixels in their respective channels. This means that the minimum value and maximum value of a color in that picture frame will not be modified. This is done for the three colors and stored. The normalization is now performed knowing the mean values, here, each pixel intensity of the channels value is found and if the value is less than the minimum value it will obtain the minimum value that was found. In the same manner, if the pixel intensity of the channel value is greater than that of the maximum value, it will obtain the maximum value found. This is done on all of the channels. Finally, all of the channels are merged back together to give the pixel block it's intensity value.

5.2 XYZ to LMS Conversion

The dehazed image is now converted to the XYZ color space. The XYZ color space is absolute color space which is the opposite of a generic color space like RGB. It is a

Tristimulus value that appeals to all the wavelengths the human can perceive. The model captures the Y as the luminance, X is a mixture of response curves that are chosen to be non-negative and Z as a quasi-equal to blue. This distribution is very helpful as setting the Y as luminance all the chromatic values can be obtained in the XZ plane at the Y value. The XYZ color space is multiplied to a chromatic adaptation matrix in the Von Kries transform method, however, this expects the LMS color space. The relationship between the XYZ and LMS color spaces is linear, so the transition is represented by a transformation matrix.

This produces the final image, in some cases there needs to be a simple color balance added to retain the color of the image or bring back some color. It also gives a saturation to the image within the parameter that is specified.

5.3 Underwater Image Quality Measurement

A measurement quality standard for grading and evaluating underwater images is being established. There are a two evaluation standards that consider different key aspects in the image. Underwater Image Quality Measurement is a non-reference Underwater Image Quality Measure (UIQM) that comprises of three image attributes namely, Underwater Image Colorfulness Measure (UICM), Underwater Image Sharpness Measure (UISM), and the Underwater Image Contrast Measure (UIConM) [45]. UICM determines its values based on the RG and YB chrominance in the color components. In UCIM the first order static mean value μ represents the chrominance intensity. A mean value that is closer to zero in the RG–YB opponent color component implies a better white balance. It carries out μ_{RG} and μ_{YB} which can be a greener tone when higher or bluer tone when lower depending on the value of μ_{RG} . The second-order statistic variance σ^2 in demonstrates the pixel activity within each color component. Greater variance in this results in higher dynamic range [46].

$$UICM = -0.0268\sqrt{\mu_{\alpha, RG}^2 + \mu_{\alpha, YB}^2} + 0.1586\sqrt{\sigma_{\alpha, RG}^2 + \sigma_{\alpha, YB}^2} \quad (5.1)$$

UISM determines the sharpness on edges in which the Sobel edge detector [47] is first applied on each RGB color component. The resultant edge map is then multiplied with the original image to get the grayscale edge map. By doing this, only the pixels on the edges from the original underwater image are preserved. This is known as Enhancement Measure Estimation (EME) [48]. The greater the vale of the UISM the more sharp the image appears to be.

$$UISM = \sum_{c=1}^3 \lambda_c EME(\text{grayscale edge}_c) \quad (5.2)$$

$$EME = \frac{2}{k_1 k_2} \sum_{l=1}^{k_1} \sum_{k=1}^{k_2} \log \left(\frac{I_{\max,k,l}}{I_{\min,k,l}} \right) \quad (5.3)$$

where the image is divided into k_1 and k_2 blocks, $(I_{\max,k,l})/(I_{\min,k,l})$ indicates the relative contrast ratio within each block and EME measures in each RGB color component.

UIConM grades the contrasts obtained in the image by using a Log to the Agaian Measure of Enhancement by Entropy (AMEE) [49] on the intensity image and gives emphasis on low lighting situations and areas with low luminance.

$$UIConM = \log AMEE(Intensity) \quad (5.4)$$

The entire generation of the UIQM is including three parameters c_1, c_2 and c_3 that are multiplied to each of the measurements above and linearly combined. Here the parameters are chosen based on the application to evaluate the performance of the image enhancement. The overall underwater image quality measure is then given by

$$UIQM = c_1 \times UICM + c_2 \times UISM + c_3 \times UIConM \quad (5.5)$$

The other standard of evaluation is the Underwater Color Image Quality Enhancement that grades the images in a sum total point system. The factors that are considered into making the sum total is the colorfulness in effect of atmospheric light (UICM) and the colorfulness with respect to quality in saturation (QSM).

$$UCIQE = c_1 \times \sigma_c + c_2 \times con_l + c_3 \times \mu_s. \quad (5.6)$$

Chapter 6

Implementation

A solution was established where there would be a real time result for the better visualization with a color corrected image for the human inspection and operators with its software implementation done with the help of the OpenCV tools in integration with Robot Operating System (ROS). The Offline processing would be done offshore once the robot had returned from its mission with the software implementation done in MatLab with the help of the OpenCV tools.

OpenCV stands for Open source Computer Vision[50] and is a library of functions aimed at computer vision. It has several hundreds of computer vision algorithms in the areas of application like 2D and 3D, facial recognition, gesture recognition, mobile robotics and object detection are some examples. OpenCV is written in C++ as its primary interface that also binds MatLab, Java and Python.

MatLab (Matrix Laboratory)[51] is a software that allows matrix manipulations, plotting of functions and data, implementing algorithms and interfacing programming languages like C,C++, Java and Python. MatLab has it's own proprietary programming language. It has a lot of important toolboxes that help create solutions like Deep Learning, Computer Vision, Signal processing, Robotics and Control Systems. The key focus is on the toolbox for Computer Vision to help achieve the implementation required [52]. It contains various algorithms and functions that can create a solution and is flexible to integrate the OpenCV tool.

6.1 Color Correction

This implementation belongs to the real time process and it is performed using OpenCV functions with the implementation in ROS.

Obtaining the image size:

The images that are being input need to have a frame size. This is the amount of pixels that the frame/image contains. To calculate this, we load the image and find out the rows

and columns that the image has. This is our image size. For example: An image can have the size of 2160x720, which means the image has about 1.5 million pixels in that frame. In our methodology we resize the image size to 600x400.

Normalization: All color images have 3 channels per pixel which store the designated values of the colors Red, Green and Blue in them. However in OpenCV the images are store as BGR. In normalization we take the image size and split the pixels into their respective rows and columns. We convert the image into its grayscale, with the help of an OpenCV function `cvtColor`, as the normalization methodology works on the illumination values in the pixels. For the case in color pictures this effects the α , β and γ values of the R, G and B. The distribution of the three channels ranges from 0 to 255, equalizing the values of each pixel in those channels is done by taking the mean of the maximum and minimum values.

$$I_{new} = (I - \min_{r,g,b}) * \frac{255}{\max - \min} \quad (6.1)$$

A filter factor of 1 is used when finding out the image intensity, as it is an ideal value which translates the most information from pixel to pixel.

Once the normalization is done the the intensity values are merged back into the original image giving an even and average distribution range to all the channels. It is sometimes also known as contrast stretching or histogram stretching.

Algorithm 1 Color Correction

Input: Raw Image

Filter Factor =1;

Output: Processed color corrected image

```
1: Read image in color and store it in a matrix
2: Resize the image according to application
3: Convert to Gray scale and obtain mean illumination value which is INTENSITY.
4: N = imagerows*imagecolumns
5: for Each row and column do
6:   Increase intensity of BGR
7:   while Minimum value of BGR >= MIN INTENSITY THRESHOLD do
8:     Move to next pixel
9:   end while
10:  while Maximum value of BGR <= MAX INTENSITY THRESHOLD do
11:    Move to next pixel
12:    if Intensity >= MAX INTENSITY THRESHOLD then
13:      Keep intensity of previous pixel
14:    end if
15:  end while
16: end for
17: for All rows and columns do
18:   For all rows and columns: If any pixel value is lesser than its minimum threshold it
   is clamped.
19:   If any pixel value is greater than its maximum threshold it is clamped.
20: end for
21: for All rows and columns do
22:   Compute the mean intensity of all channels respectively
23: end for
24: return Normalized color image
25: Use a sharpness mask to obtain a clearer image
26: Apply Guassian Blur
27: Remove the amount of blur from original image
28: return Color Corrected Image
```

In the algorithm 1 the N is the total number of pixels by multiplying the rows and columns of the image. We find out the the intensity values of each independent color channel. It is calculated as BGR because of the function imread. The minimum and maximum intensity values obtained and stored of each color channel.

A sharpness filter is applied to remove any blurring on the image, which is added using

the OpenCV function of Gaussian Blur. This function creates a blur around the edges and corners of the image which depends on the kernel size, the deviation of the kernel in X-direction, and the deviation of the kernel in Y-direction. The blurred image generated is subtracted and from the normalized image while keeping its absolute difference less than a threshold that is set by the user. In our case the threshold was set to 5 to achieve the best results. The image is sharpened by taking the normalized image and multiplying the value of sharpness to it, adding the blurred image and multiplying the negative of that value.



Figure 6.1: Color Correction

Another approach was experimented on which gave very similar results, which was, taking the image and converting it into its L^*A^*B planes and applying the CLAHE algorithm [53] to the Luminosity (L) channel of that image. The modifications are performed on the L channel with a clipping limit of 0.53 and then merged back into the RGB color space to give us the result.

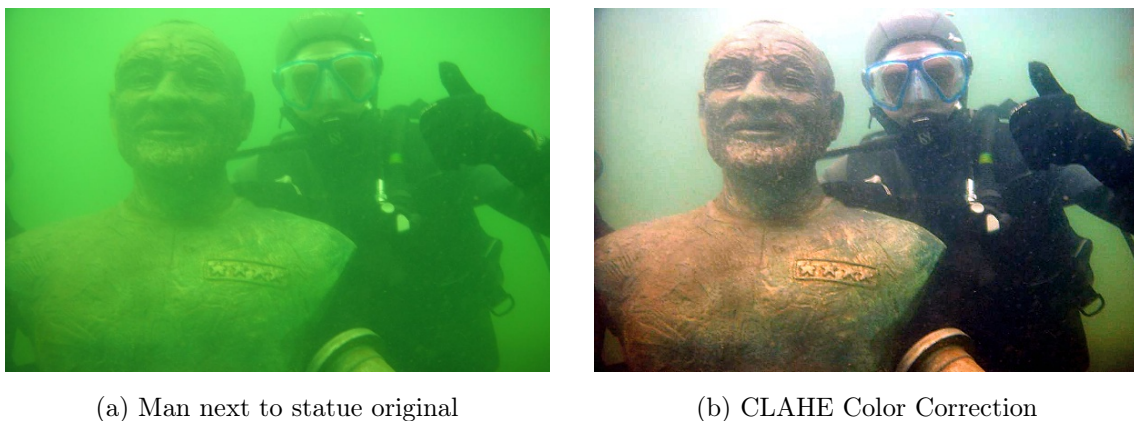


Figure 6.2: Color Correction using CLAHE

As we can see from the figures 6.1 and 6.2 with the CLAHE methodology there is

a stronger halo around the pure white regions. Changing the clipping limit changes the entire images luminosity and not just that specific region.

6.2 Dark Channel Prior

DCP is a haze removal method that was adapted into underwater imaging. When applied by itself without any color rectification to underwater images it has an appearance like in figure 6.3.



(a) Man next to statue original



(b) Applying Dark Channel Prior only

Figure 6.3: Dark Channel Prior Filtering

DCP calculates the dark pixels of an image. Those dark pixels are the reference limit to be removed from the image and are taken out. Since the images are underwater an assumption of the airlight is taken matching the nature of the outside world. The dark channel pixels are taken and masked with those values to rectify the dark pixels that exist and are freed from the image to be transmitted. The transmission of the pixels are normalized with the values of the pixels that are not dark pixels with the constraints that were applied during airlight. It is made sure here in the recovery that there is no pixel values are exceeding the range of 255. If any pixels tend to be in that state it is brought down to 255. This entire process then produces a dehazed image were the foggy nature has been completely removed from the image.

Algorithm 2 Dark Channel Prior Algorithm

Input: Image (color corrected)

```
1: Detection of dark pixels- Pixels with the lowest intensity
2: for Each pixel x in Red Channel Original (ROG) ROG(x) do
3:   Store the dark pixels values in Jdark_red(x)
4: end for
5: for Each pixel x in Green Channel Original (GOG) GOG(x) do
6:   Store the dark pixels values in Jdark_green(x)
7: end for
8: for Each pixel x in Blue Channel Original (BOG) BOG(x) do
9:   Store the dark pixels values in Jdark_blue(x)
10: end for
11: for Each RGB Channel do
12:   Pixel_r,g,b(x)=P(x)-Jdark_red,green,blue(x)
13: end for
14: Assume airlight or atmospheric light A
15: for Each channel pixel value do
16:   Red(x)=A.Jdark_red
17:   Green(x)=A.Jdark_green
18:   Blue(x)=A.Jdark_blue
19: end for
20: //Denoting airlight values as a part of transmission t
21: //Applying transmission and the merged values on to each channel of the image
22: for Each pixel x do
23:   if ROG(x) < Red(x) then
24:     Rfinal=Red(x)
25:   else
26:     Rfinal=ROG(x)
27:   end if
28:   if GOG(x) < Green(x) then
29:     Gfinal=Green(x)
30:   else
31:     Gfinal=GOG(x)
32:   end if
33:   if BOG(x) < Blue(x) then
34:     Bfinal=Blue(x)
35:   else
36:     Bfinal=BOG(x)
37:   end if
38: end for
39: return Dehazed Image                48 (Rfinal,Gfinal,Bfinal)
```

where $J_{\text{dark}}(x)$ is the dark channel prior of the pixel x .

6.3 XYZ to LMS conversion

The dehazed image is now converted to the XYZ color space and multiplied to a chromatic adaptation matrix in the von Kries transform method, however, this expects the LMS color space. The relationship between the XYZ and LMS color spaces is linear, so the transition is represented by a transformation matrix.

$$\begin{bmatrix} L \\ M \\ S \end{bmatrix} = \begin{bmatrix} 0.3897 & 0.6889 & -0.0786 \\ -0.2298 & 1.1834 & 0.0464 \\ 0.0000 & 0.0000 & 1.0000 \end{bmatrix} \begin{bmatrix} X \\ Y \\ Z \end{bmatrix} \quad (6.2)$$

There is no defined transition matrix which is a perfect example for any specific application, some images can utilise a different transition matrix and yield a better result. For our case we chose the von Kries matrix as it deals with the chromatic adaptation and helps the image from becoming over saturated or contaminated with other artificial colors.



(a) Man next to statue original



(b) Final processed Image



(c) Final processed image with color balance



(d) Final image with added sharpness

Figure 6.4: LMS converted Final Images

6.4 Integration in Robot Operating System-ROS

The integration with ROS can be seen in figure 6.5. The entire process is split into two parts. The real time processing accesses the camera topic, `image_compressed`, from the robot which is published from the ROS camera node. That topic is enhanced by the color correction algorithm which behaves as a node, which subscribes to the topic and publishes an output topic. The output topic can be accessed from the image viewer or a Graphical User Interface (GUI) of the system for the human operates to see real time image enhanced image data.

The output topic saves the images that are obtained for later post processing offline or offshore when the robot returns from its mission. This images can be transferred on to another computer with a higher performance to provide a faster result. These images are then accessed and the DCP and LMS conversion is applied to the image which can be published to a topic or as an output, which can used for feature extraction, as a dataset for neural networks, implemented along with super resolution and other processes.

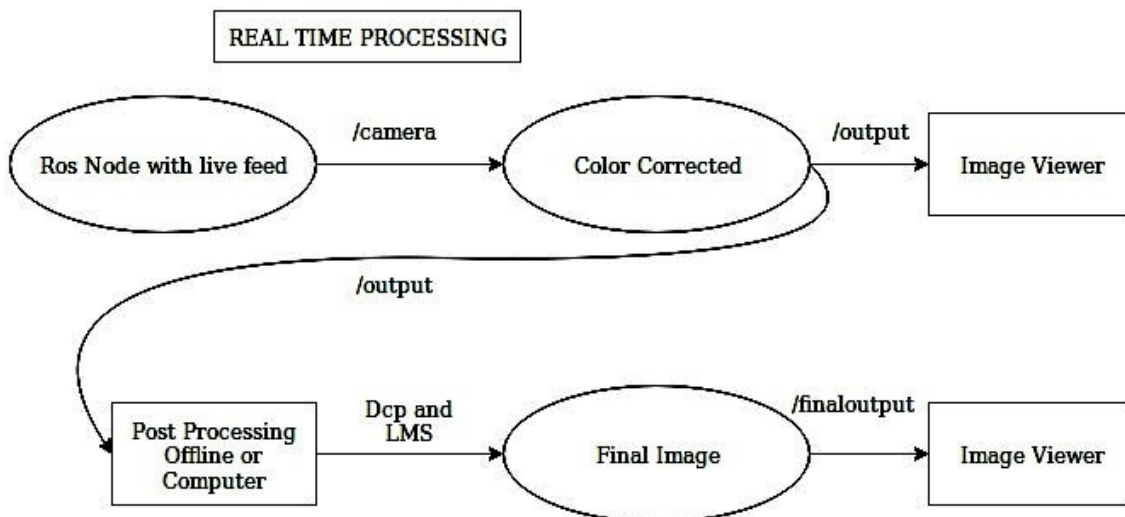


Figure 6.5: ROS functionality of the process

Chapter 7

Results

The proposed strategy was tested for real underwater videos and images taken from the missions. The UX1 robot provides the data-sets that are a part of this thesis. The high quality images which are used, are taken from live, real world, mining grounds. For testing purposes, the data-set is comprised of images taken from previous missions in the Idrija mines as seen in figure 7.1. As a result, images and videos have been captured using various cameras and setups. The robot is available in LSA there was ease of access and availability of images which were stored in a rosbag which could be used to extract the images or directly fed as an input for ros node.



Figure 7.1: UX1 Robot deployment in mine shaft with reduced visibility[11]

The data sets collected and worked upon are different target oriented images as seen below in figure 7.2 to figure 7.10 for a vast variety to prove the methodology works in

such real scenarios. A lot of images contain important information that is key in feature extraction or object detection.

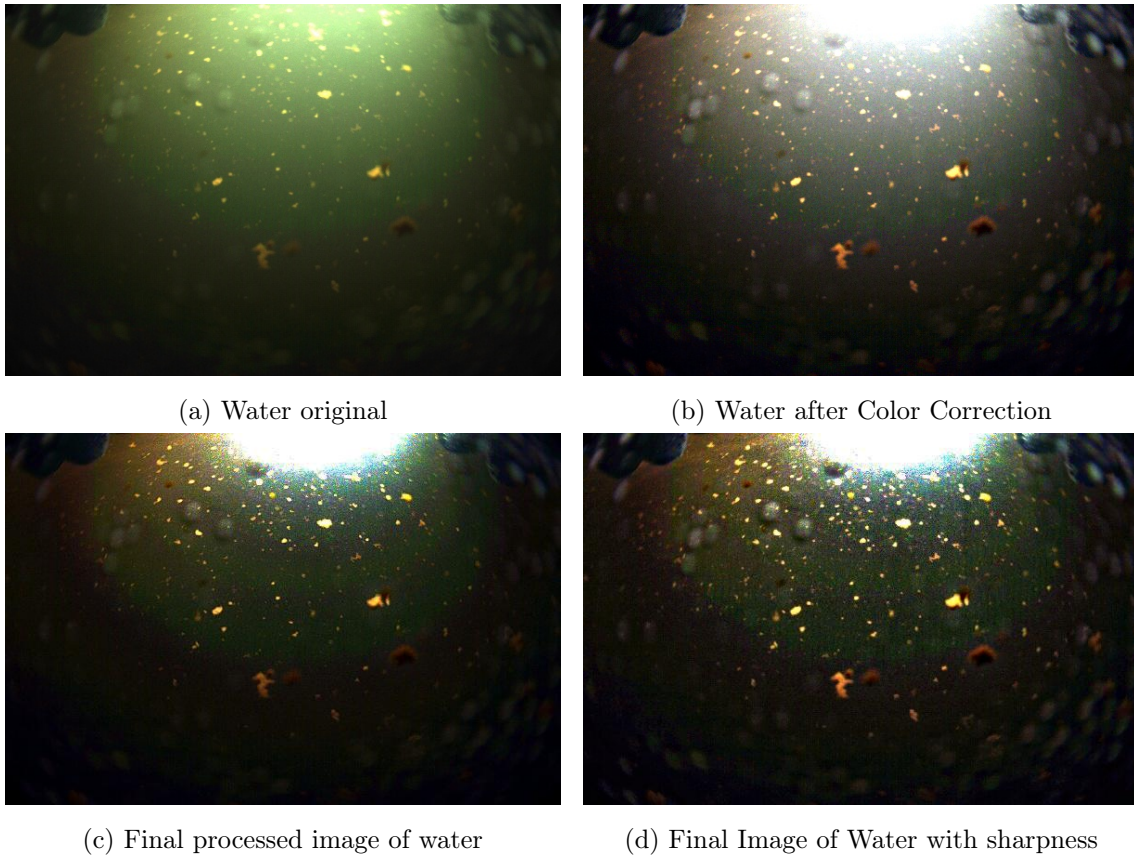


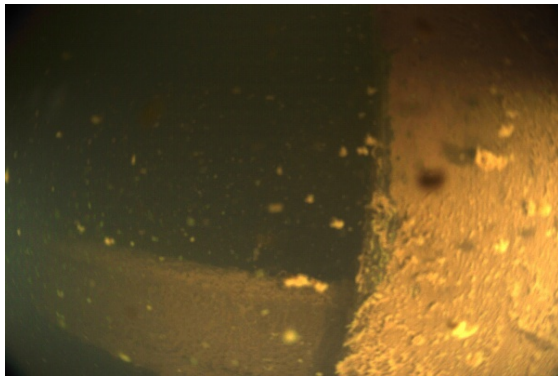
Figure 7.2: Water

The enhancement of the water shows some improvements where detection of the water particles that are floating are clearer visible. We also see the air bubbles that are formed due to the pressure under water which can be eradicated with more time the robot spends underwater and polishing the camera dome which is made of glass.

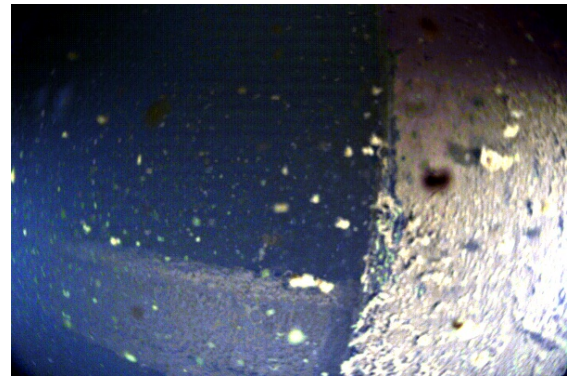
The wall with the structure in figure 7.3 is seen by the camera after moving close to it, the other sensors in the robot stop it from colliding with the wall and the recorded images shows a lot of floating particles but a clear distinction is seen.

Since the image has more saturation or warmth in the image than any other characteristic it is cooled off after color correction. After the dehazing and conversion to the LMS color space we can some color return back into the image giving the wall its muddy, mossy look and cover. With the sharpness filter being applied the final result picks up all the floating particles that are in front of the camera and giving it more definition.

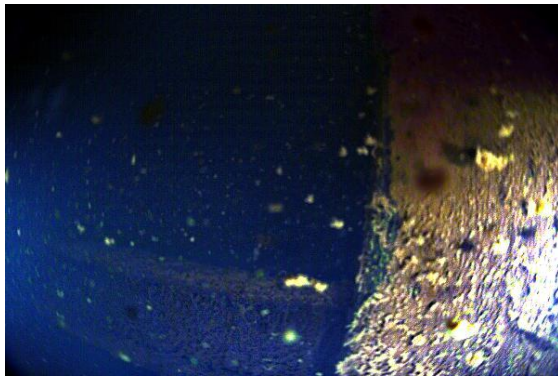
The seafloor in figure 7.4 with a lot of dirt was one of the worst case scenarios to process, as the saturation is very high in the image it is difficult for the algorithm to feed the correct values into the image.



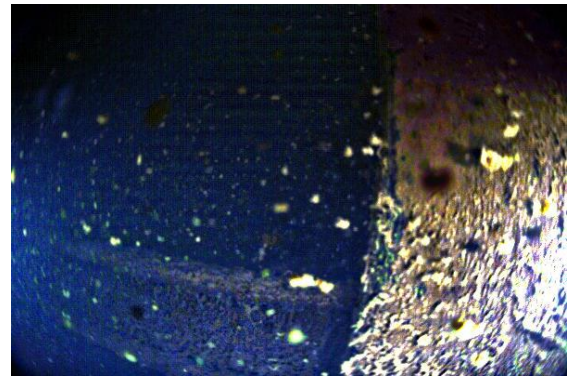
(a) Wall original



(b) Wall after Color Correction

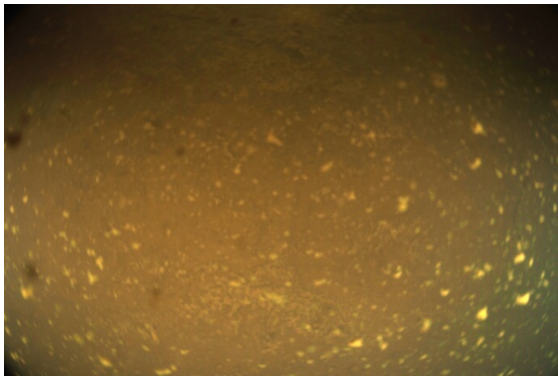


(c) Final processed image of wall

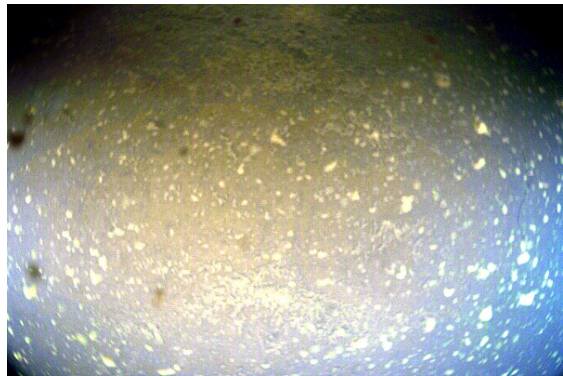


(d) Final image of Wall with sharpness

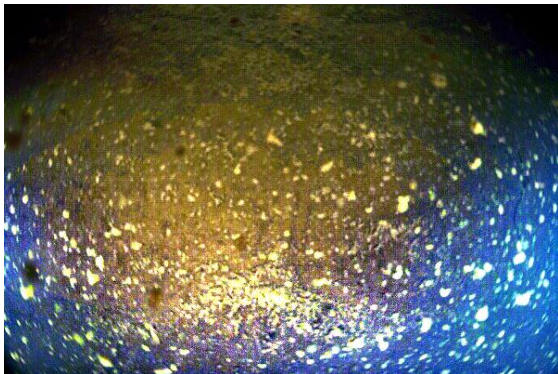
Figure 7.3: Wall with a Structure



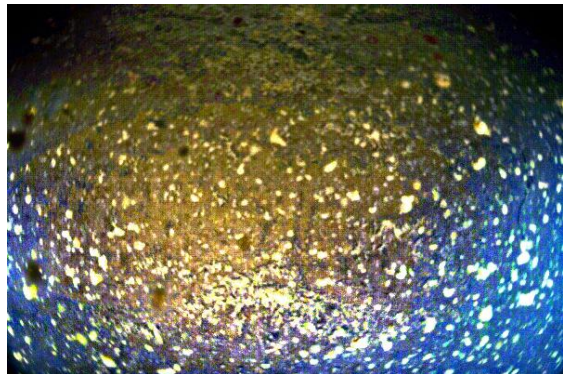
(a) Seafloor



(b) Seafloor after Color Correction



(c) Final processed image of the seafloor



(d) Sharpened Image of Seafloor

Figure 7.4: Seafloor

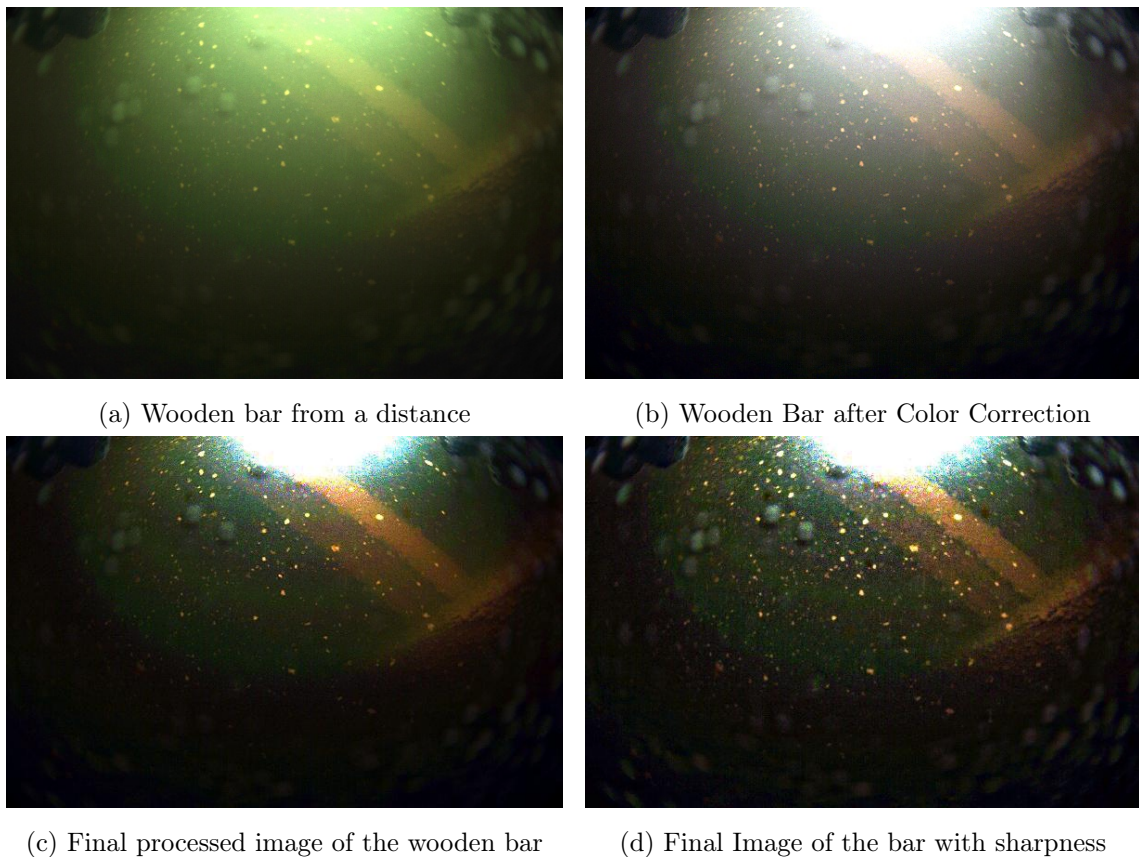


Figure 7.5: Wooden Bar from a distance

The wooden bar from a distance in figure 7.5 has better visualization when it is closer to the object. From the image we can see that the pipe is detectable.

A wooden bar as seen in figure 7.6 taken close up provides a better identification of the structure and its details.

Two wooden bars one under the other in figure 7.7, looks like the other bar is barely visible, after enhancement the second bar can be seen underneath.

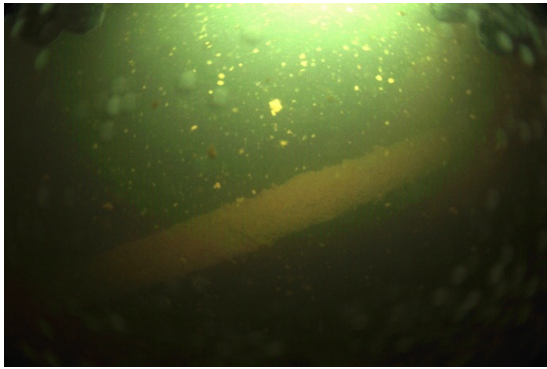
A structural beam in figure 7.8 with mud or moss on it.

A school of fish as seen in figure 7.9 and its color details are highlighted with a much clearer vision for detection.

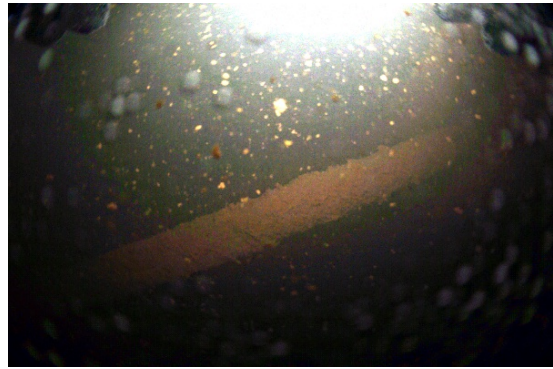
Colored fish with corals behind them in figure 7.10 have a very clear color and detailing to it.

In the figure 7.11, the robot's camera captures the image on the left and outputs the real-time processed image on the right.

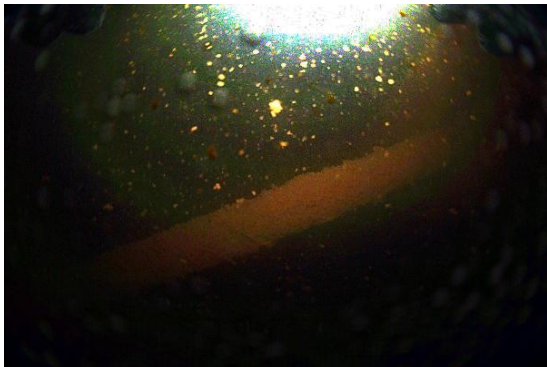
This significantly improves the vision to detect obstacles, identify resources and improve its navigation and help the remote user with a better quality image making it easier to spot different minerals.



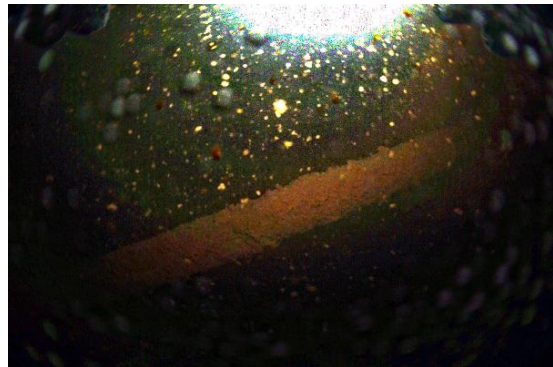
(a) A Wooden Bar



(b) Bar after Color Correction

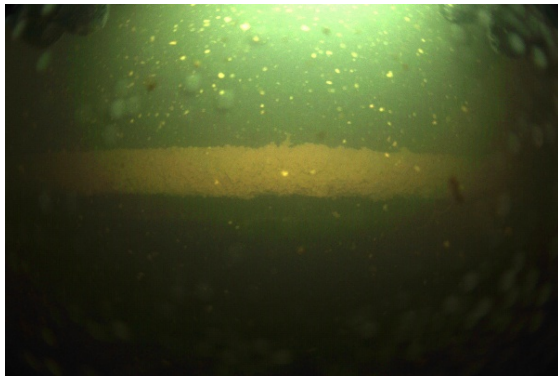


(c) Final processed image of the Bar



(d) Final Image of the Bar with sharpness

Figure 7.6: A Wooden Bar



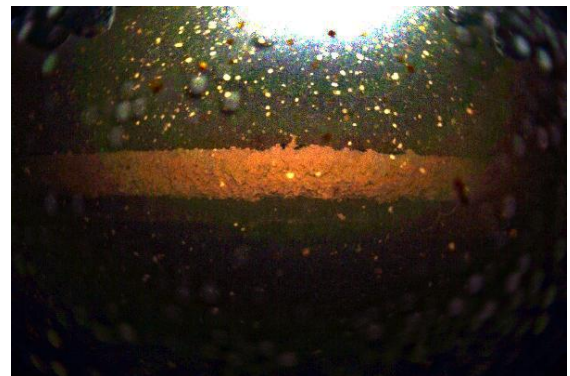
(a) Two bars one under the other



(b) Two Bars after Color Correction

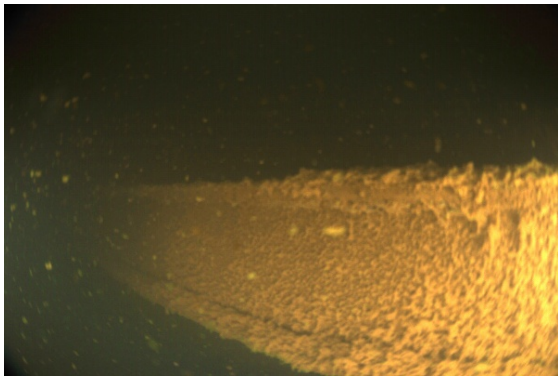


(c) Final processed image of the bars

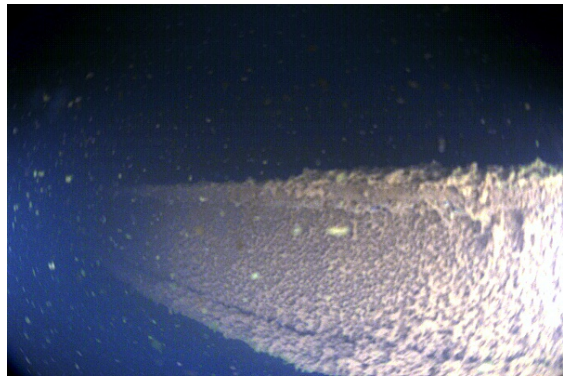


(d) Final Image of the bars with sharpness

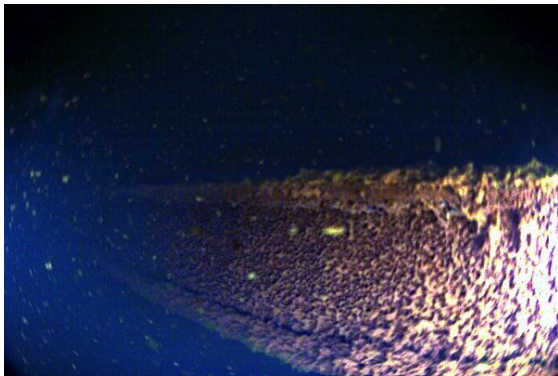
Figure 7.7: Two wooden bars one under the other



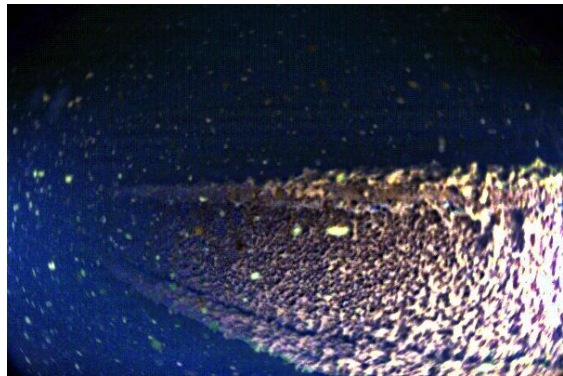
(a) A Beam



(b) Beam after Color Correction

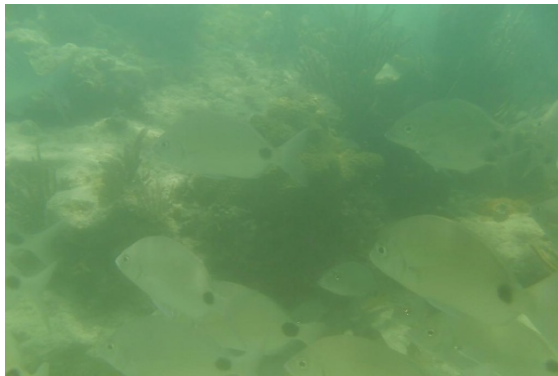


(c) Final processed image of the Beam



(d) Final Image of the Beam with sharpness

Figure 7.8: A Structural beam



(a) A school of fish



(b) Fish after Color Correction



(c) Final processed image of the school of fish



(d) Final Image of the fish with sharpness

Figure 7.9: A school of fish



(a) Colored fish with corals



(b) Fish after Color Correction



(c) Final processed image of the school of fish



(d) Final Image of the fish with sharpness

Figure 7.10: Colored fish with corals

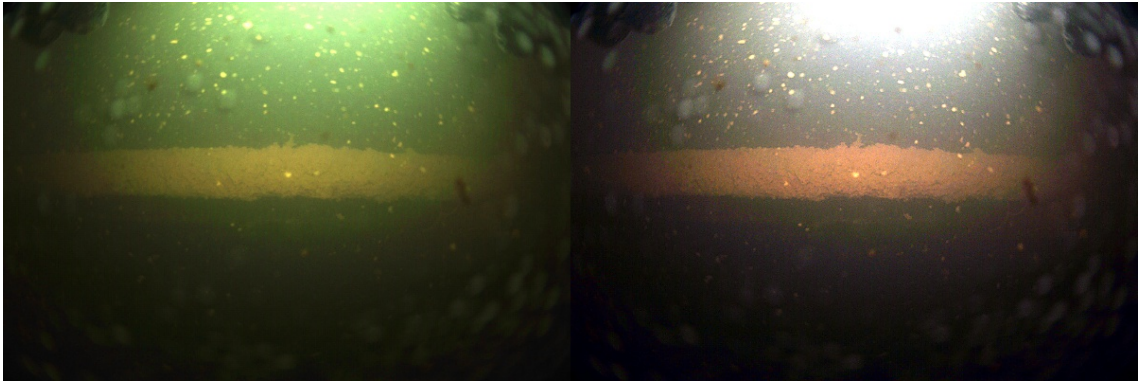
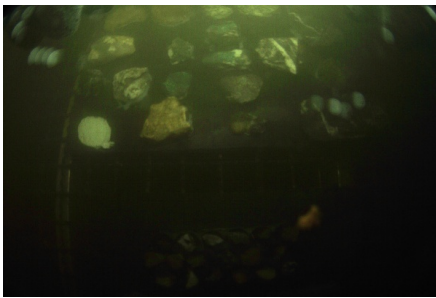


Figure 7.11: Left-Original image, Right-Color corrected image from the ros node

The mineral sample board enhancement shows the difference in the colors between the rocks which can be spotted very easily. The characteristics of the rocks stand out compared to the original image viewed from the camera of the robot.



(a) Mineral board original



(b) Mineral board after Color Correction



(c) Final processed image of Mineral board

Figure 7.12: Mineral Sample board

Our technique is computationally effective taking approximately 0.36 seconds (ROS node code) for a 600 x 400 frame i.e, the color correction implementation only. The original size of the image 2056 x 1544. The image has to be resized for a faster computation, as that produces an optimized implementation for the results that could be achieved in real-time on common hardware. The Matlab implementation is done on the R2016a version and takes approximately 1.6 seconds for the resolution of 600x400. In total our entire

methodology would take about 2 seconds for each frame to give us the final result. Since the latter half requires more time and processing by the robot is not an immediate real time solution, it is done offline. All methods are implemented on a laptop with a 3.10GHz, i7-6500 CPU. The time taken for each part of our method is mentioned below:

Table 7.1: Timing-Table

Original Image (600x400)	Color Corrected	DCP	Final result
Time(in s)	0.36	1.29	0.43

The comparison between the test images on the UIQM (considering only the contrast and sharpness) and Underwater Color Image Quality Evaluation (UCIQE) which is another standard metric are given in the table below:

Table 7.2: Quality Measurement Table Original

Final Result Values	Variance Chroma	Mean Saturation	UCIQE
Mineral Sample Board Original	11.5779	0.3989	27.6178
Man next to Statue Original	8.8451	0.6954	21.4889
Fishes with Corals Original	3.5901	0.4275	19.8072
A beam Original	16.9705	0.5518	34.8010
The seafloor Original	9.5755	0.6417	31.3836

Table 7.3: Quality Measurement Table

Final Result Values	Variance Chroma	Mean Saturation	UCIQE
Mineral Sample Board	9.8910	0.4815	32.2030
Man next to Statue	19.0581	0.6825	36.5450
Fishes with Corals	14.6543	0.6831	34.4842
A beam	13.6307	0.6173	33.9882
The seafloor	16.1692	0.5440	35.1573

From the values seen above the resulting images are above the 28 point value for UCIQE standard.

Here we can see the comparison between the original and enhanced images. We can note that in some situations like the seafloor where there is a higher saturation which is equalised in the enhanced image.

Chapter 8

Conclusion and Future Work

8.1 Conclusion

In conclusion, our methodology proves to be efficient to be used in real time scenarios and provide substantial results for underwater robots in the mining application. The objectives that the project proposed, was accomplished in the respective areas. We successfully identified the problems within the images which was the color cast and hazing problems which were solved with the development of the algorithm. The solution proposed is a real time algorithmic solution to normalise the color and enhance underwater images to be able to extract more information and make it visibly clearer for the purpose of underwater mining for both the human visual and the robots processing for detection. The post processing which is done offline helps in obtaining better features and extraction of data. The method was tested with a variety of images from a dataset. All the experiment results taken in real scenarios demonstrate that our method is in genuine color, has natural appearance. The validation of the images used from the real life datasets were up to par with the grading benchmark that exists.

This technology developed in the context of this dissertation has resulted in the publication of an IEEE conference paper, in the IEEE/MTS OCEANS 2019 conference, Marseille, France, held in June 2019.

8.2 Future Work

Our method, even despite down-scaling can further be enhanced and has the potential to yield even better results by using the method of Super Resolution.

The Dark channel Prior automation is done using an estimation value for the first frame which needs to be tracked as the parameter is relevant for each frame in the video storing the values for each frame sequentially.

**THIS PAGE
INTENTIONALLY
LEFT BLANK**

References

- [1] Norval Strachan. “Recognition of fish species by color and shape”. In: *Image and Vision Computing* 11 (Feb. 1993), pp. 2–10. DOI: 10.1016/0262-8856(93)90027-E.
- [2] Rick Docksai. “A Future for Global Sea Life”. In: *World Future Review* 3 (May 2011), pp. 70–72. DOI: 10.1177/194675671100300209.
- [3] Shiela Marcos, Maricor Soriano, and Caesar Saloma. “Classification of coral reef images from underwater video using neural networks”. In: *Optics express* 13 (Nov. 2005), pp. 8766–71. DOI: 10.1364/OPEX.13.008766.
- [4] Raimondo Schettini and Silvia Corchs. “Underwater Image Processing: State of the Art of Restoration and Image Enhancement Methods”. In: *EURASIP Journal on Advances in Signal Processing* 2010.1 (Apr. 2010). ISSN: 1687-6180. DOI: 10.1155/2010/746052. URL: <https://doi.org/10.1155/2010/746052>.
- [5] M. Dunbabin, B. Lang, and B. Wood. “Vision-based docking using an autonomous surface vehicle”. In: *2008 IEEE International Conference on Robotics and Automation*. May 2008, pp. 26–32. DOI: 10.1109/ROBOT.2008.4543182.
- [6] *VAMOS!* <http://vamos-project.eu>.
- [7] A. Martins et al. “EVA a Hybrid ROV/AUV for Underwater Mining Operations Support”. In: *2018 OCEANS - MTS/IEEE Kobe Techno-Oceans (OTO)*. May 2018, pp. 1–7. DOI: 10.1109/OCEANSKOBE.2018.8558880.
- [8] F. Lopes et al. “Structured light system for underwater inspection operations”. In: *OCEANS 2015 - Genova*. May 2015, pp. 1–6. DOI: 10.1109/OCEANS-Genova.2015.7271564.
- [9] Angelos Mallios et al. “Toward autonomous exploration in confined underwater environments”. In: *Journal of Field Robotics* (Nov. 2015), n/a–n/a. DOI: 10.1002/rob.21640.
- [10] *unexmin*. <https://www.unexmin.eu>.
- [11] A. Martins et al. “UX 1 system design - A robotic system for underwater mining exploration”. In: *2018 IEEE/RSJ International Conference on Intelligent Robots and Systems (IROS)*. Oct. 2018, pp. 1494–1500. DOI: 10.1109/IROS.2018.8593999.

- [12] Kashif Iqbal et al. “Underwater Image Enhancement Using an Integrated Colour Model”. In: *IAENG International Journal of Computer Science* 34 (Jan. 2007).
- [13] Ramandeep Kaur and Dipen Saini. “Image Enhancement of Underwater Digital Images by Utilizing $L^*A^*B^*$ Color Space on Gradient and CLAHE based Smoothing”. In: *Communications on Applied Electronics* 4 (Apr. 2016), pp. 22–30. DOI: 10.5120/cae2016652166.
- [14] Gianfranco Bianco et al. “A New Color Correction Method For Underwater Imaging”. In: *The International Archives of the Photogrammetry, Remote Sensing and Spatial Information Sciences, Volume XL-5/W5*. Apr. 2015. DOI: 10.5194/isprsarchives-XL-5-W5-25-2015.
- [15] W. Zhang, G. Li, and Z. Ying. “A new underwater image enhancing method via color correction and illumination adjustment”. In: *2017 IEEE Visual Communications and Image Processing (VCIP)*. Dec. 2017, pp. 1–4. DOI: 10.1109/VCIP.2017.8305027.
- [16] Anya C Hurlbert and Christopher JL Wolf. “Contribution of local and global contrasts to color appearance: a Retinex-like model”. In: *Human Vision and Electronic Imaging VII*. Vol. 4662. International Society for Optics and Photonics. 2002, pp. 286–297.
- [17] E. Park and J. Sim. “Gradient-based contrast enhancement and color correction for underwater images”. In: *2017 Asia-Pacific Signal and Information Processing Association Annual Summit and Conference (APSIPA ASC)*. Dec. 2017, pp. 1444–1447. DOI: 10.1109/APSIPA.2017.8282259.
- [18] M. S. Hitam et al. “Mixture contrast limited adaptive histogram equalization for underwater image enhancement”. In: *2013 International Conference on Computer Applications Technology (ICCAT)*. Jan. 2013, pp. 1–5. DOI: 10.1109/ICCAT.2013.6522017.
- [19] “A hybrid method for underwater image correction”. In: *Pattern Recognition Letters* 94 (2017), pp. 62–67. ISSN: 0167-8655. DOI: <https://doi.org/10.1016/j.patrec.2017.05.023>. URL: <http://www.sciencedirect.com/science/article/pii/S016786551730171X>.
- [20] C. Ancuti et al. “Enhancing underwater images and videos by fusion”. In: *2012 IEEE Conference on Computer Vision and Pattern Recognition*. 2012, pp. 81–88. DOI: 10.1109/CVPR.2012.6247661.
- [21] K. He, J. Sun, and X. Tang. “Single Image Haze Removal Using Dark Channel Prior”. In: *IEEE Transactions on Pattern Analysis and Machine Intelligence* 33.12 (Dec. 2011), pp. 2341–2353. ISSN: 0162-8828. DOI: 10.1109/TPAMI.2010.168.

- [22] R. Sathya, M. Bharathi, and G. Dhivyasri. “Underwater image enhancement by dark channel prior”. In: *2015 2nd International Conference on Electronics and Communication Systems (ICECS)*. Feb. 2015, pp. 1119–1123. DOI: 10.1109/ECS.2015.7124757.
- [23] C. O. Ancuti et al. “Locally Adaptive Color Correction for Underwater Image Dehazing and Matching”. In: *2017 IEEE Conference on Computer Vision and Pattern Recognition Workshops (CVPRW)*. July 2017, pp. 997–1005. DOI: 10.1109/CVPRW.2017.136.
- [24] Saeed Anwar, Chongyi Li, and Fatih Porikli. “Deep Underwater Image Enhancement”. In: *CoRR* abs/1807.03528 (2018). arXiv: 1807.03528. URL: <http://arxiv.org/abs/1807.03528>.
- [25] N. Jerlov. *Marine Optics*. Vol. 14. Jan. 1976.
- [26] Diederik Kingma and Jimmy Ba. “Adam: A Method for Stochastic Optimization”. In: *International Conference on Learning Representations* (Dec. 2014).
- [27] *Spectra of Pantone Colors*. Licensed Under Creative Commons.
- [28] Ewald Hering. “Outlines of a Theory of the light sense”. In: *Sitzber. Wiener. Akad.* 66 (Jan. 1878).
- [29] *NCS Color Model*. Licensed Under GNU Free Documentation License and Creative Commons.
- [30] *Adobe RGB Color Model*. Licensed Under GNU Free Documentation License and Creative Commons.
- [31] Bernice Rogowitz, Thrasyvoulos Pappas, and Scott J. Daly. “Human Vision and Electronic Imaging XII”. In: *Proceedings of SPIE - The International Society for Optical Engineering* (Mar. 2007).
- [32] *RGB Color Model*. Released to the public domain by its Author, SharkD.
- [33] Mark Fairchild. “Color Appearance Models”. In: *Proceedings of SPIE - The International Society for Optical Engineering* (June 2002).
- [34] *Four Different "lightness" Conditions*. Licensed Under GNU Free Documentation License and Creative Commons.
- [35] *Normalized responsivity spectra of human cone cells, S, M, and L types*. Licensed Under GNU Free Documentation License and Creative Commons.
- [36] Mark Fairchild. “A revision of CIECAM97s for practical applications”. In: *Color Research and Application - COLOR RES APPL* 26 (Dec. 2001). DOI: 10.1002/col.1061.

- [37] “Image technology colour management — Architecture, profile format, and data structure”. In: *Specification ICC.1:2010 (Profile version 4.3.0.0)* (Apr. 2016). ISO Standard.
- [38] Pascal Getreuer. “Automatic Color Enhancement (ACE) and its Fast Implementation”. In: *Image Processing On Line* 2 (Nov. 2012), pp. 266–277. DOI: 10.5201/ipo1.2012.g-ace.
- [39] Nicolas Limare et al. “Simplest Color Balance”. In: *Image Processing On Line* 1 (Oct. 2011). DOI: 10.5201/ipo1.2011.11mps-scb.
- [40] Juan F. Molina et al. “Color and size image dataset normalization protocol for natural image classification: A case study in tomato crop pathologies”. In: Sept. 2013, pp. 1–5. ISBN: 978-1-4799-1120-2. DOI: 10.1109/STSIVA.2013.6644938.
- [41] H. Koschmeider. “Therie der horizontalen sichtweite”. In: *Beitr. Phys. Freien Atmosph.* 12 (Jan. 1924).
- [42] Raanan Fattal. “Single image dehazing”. In: *ACM Trans. Graph.* 27 (Aug. 2008). DOI: 10.1145/1399504.1360671.
- [43] M.S. Achmad et al. “Tele-Operated Mobile Robot for 3D Visual Inspection Utilizing Distributed Operating System Platform”. In: *International Journal of Vehicle Structures and Systems* 9 (Sept. 2017). DOI: 10.4273/ijvss.9.3.12.
- [44] S. Cousins. “Welcome to ROS Topics [ROS Topics]”. In: *IEEE Robotics Automation Magazine* 17.1 (Mar. 2010), pp. 13–14. DOI: 10.1109/MRA.2010.935808.
- [45] K. Panetta, C. Gao, and S. Agaian. “Human-Visual-System-Inspired Underwater Image Quality Measures”. In: *IEEE Journal of Oceanic Engineering* 41.3 (July 2016), pp. 541–551. ISSN: 0364-9059. DOI: 10.1109/JOE.2015.2469915.
- [46] J. Åhlén, D. Sundgren, and E. Bengtsson. “Application of underwater hyperspectral data for color correction purposes”. In: *Pattern Recognition and Image Analysis* 17.1 (Mar. 2007), pp. 170–173. ISSN: 1555-6212. DOI: 10.1134/S105466180701021X. URL: <https://doi.org/10.1134/S105466180701021X>.
- [47] A. Jain et al. “Comparison of edge detectors”. In: *2014 International Conference on Medical Imaging, m-Health and Emerging Communication Systems (MedCom)*. Nov. 2014, pp. 289–294. DOI: 10.1109/MedCom.2014.7006020.
- [48] Karen Panetta and Arash Samani. “Choosing the Optimal Spatial Domain Measure of Enhancement for Mammogram Images”. In: *International journal of biomedical imaging* 2014 (Aug. 2014), p. 937849. DOI: 10.1155/2014/937849.
- [49] K. Panetta et al. “Parameterized Logarithmic Framework for Image Enhancement”. In: *IEEE Transactions on Systems, Man, and Cybernetics, Part B (Cybernetics)* 41.2 (Apr. 2011), pp. 460–473.

- [50] *OpenCV*. <https://opencv.org>.
- [51] *MatLab*. <https://www.mathworks.com>.
- [52] *MatLab Image and Video Processing Tool Box*. <https://www.mathworks.com/solutions/image-video-processing.html>.
- [53] Stephen M. Pizer et al. “Adaptive Histogram Equalization and Its Variations”. In: *Computer Vision, Graphics, and Image Processing* 39 (Sept. 1987), pp. 355–368. DOI: 10.1016/S0734-189X(87)80186-X.